JOURNAL OF GEOPHYSICAL RESEARCH, VOL. 91, NO. B10, PAGES 10,203–10,228, SEPTEMBER 10, 1986

Observations of Anomalous Splitting and Their Interpretation in Terms of Aspherical Structure

MICHAEL RITZWOLLER, GUY MASTERS, AND FREEMAN GILBERT

Institute of Geophysics and Planetary Physics, Scripps Institution of Oceanography, University of California, San Diego, La Jolla

The problem of inverting for the aspherical structure of the earth is complicated by the nonlinear dependence of low-frequency seismic waveforms on aspherical structure. In an attempt to overcome this obstable, we report on the application of two complementary techniques. The first, a data space technique called singlet stripping, which linearly recombines seismic recordings to estimate singlet resonance functions, has been applied to 190 International Deployment of Accelerometers and Global Digital Seismographic Network recordings from five large events. More than 290 singlets from 34 low harmonic degree multiplets appear to have been resolved. A subset of these measurements has been compared with those produced from the second technique, a nonlinear regression, which iteratively estimates coefficients which are linear functionals of aspherical structure. Both techniques agree that most multiplets are normally split, with singlet frequency distributions insignificantly different from those predicted for a rotating, hydrostatic (RH) earth model. The main result of this paper is that both techniques also agree that approximately a third of the multiplets are anomalously split, some of which span frequency bands up to 2.5 times greater then predicted for an RH model. All of the anomalously split multiplets are SKS, PKP, or PKIKP equivalent. The observation of anomalously widely split multiplets is highly robust and provides compelling evidence for the existence of deep large-scale, nonhydrostatic aspherical structure. The inverse problem for the axisymmetric part of aspherical structure has been performed in the hope of illuminating anomalous splitting. Unless a large amount of structure in the core is included, we are unable to construct a smooth axisymmetric model which accurately predicts the splitting characteristics for the anomalous multiplets while simultaneously fitting the normally split multiplets. The location and nature of this core heterogeneity are unclear, but we find that a simple outer core structure is sufficient to give a reasonable fit to the data. There are good theoretical reasons for believing that such nonhydrostatic outer core structure is geophysically unreasonable, yet differential travel time data sensitive to core structure apparently require similar large scale heterogeneity in the core. Although this dilemma remains unresolved, spectral fitting techniques like the nonlinear regression can be applied to many more multiplets than considered here and it is not unreasonable to predict that reliable large scale aspherical models of the deep earth soon will become available.

1. INTRODUCTION

In the last 5 years, seismologists have begun to discern the large-scale, aspherical structure of the earth. *Masters et al.* [1982] showed that the observed peak shifts of fundamental spheroidal multiplets display a geographical pattern which is predominantly of harmonic degree 2. This pattern can be explained most simply by a degree 2 structure located in the transition zone of the earth. Subsequent work has used surface wave dispersion [*Nakanishi and Anderson*, 1983, 1984] and waveform modeling [*Woodhouse and Dziewonski*, 1984] to construct more complicated models of aspherical structure of the upper mantle. The aspherical structure of the lower mantle has been studied with large travel time data sets [*Clayton and Comer*, 1983; *Dziewonski*, 1984]. None of the models presented to date contain boundary perturbations or aspherical structure in the core. Direct comparison of these models yields the sort of agreement expected in the early stages of large research programs: qualitative agreement at degrees 2 and 3 for the lower mantle models [*Hager et al.*, 1985] and a similar agreement of "many features of (the) maps" [*Woodhouse and Dziewonski*, 1984] for the upper mantle models. It has been recognized for some time that the detailed study of the splitting characteristics of low-frequency multiplets in the earth's free oscillation spectrum could provide constraints on whole earth aspherical structure complementary to those mentioned above. A first step toward such a detailed study is the subject of the current paper.

Splitting of the free oscillations of the earth, caused by rotation and slight departures of the earth from sphericity, was first observed nearly a quarter of a century ago [*Ness et al.*, 1961; *Benioff et al.*, 1961]. These observations stimulated theoretical work which has led to a fairly complete understanding of the phenomenon [*Backus and Gilbert*, 1961; *Pekeris et al.*, 1961; *Dahlen*, 1968, 1969, 1976; *Zharkov and Lyubimov*, 1970; *Madariaga*, 1971; *Luh*, 1973, 1974; *Woodhouse* 1976, 1980; *Stein and Geller*, 1978; *Woodhouse and Dahlen*, 1978]. It is now possible to compute the singlet frequencies and eigenfunctions for earth models with quite general types of aspherical perturbations [*Masters et al.*, 1983; *Tanimoto and Bolt*, 1983; *Morris et al.*, 1984; *Park and Gilbert*, 1986]. The number of observations of splitting has remained small because most multiplets do not span frequency bands broad enough to allow the discrimination of individual singlets from single recordings. The development of multiple taper spectral techniques [*Thomson*, 1982; J. Park et al., unpublished manuscript, 1986; C. Lindberg and J. Park, unpublished manuscript, 1986] may help alleviate this problem, but many high-quality seismic recordings are required to iso-

Paper number 5B5642.
0148-0277/86/005B-5642$05.00

late individual singlets within all but a very few multiplets. Thus it was only with the installation of global digital seismic arrays in the mid-1970s that we were provided with the means to resolve many singlets.

It is often convenient to reference observations of splitting to the frequencies predicted for a rotating earth model in hydrostatic equilibrium. Such a model (hereafter referred to as an RH model) includes the effects of rotation and ellipticity as calculated by Clairaut's theory. Because an RH model possesses axisymmetric asphericity, the singlet eigenfunctions of an uncoupled multiplet can be written, in a spherical coordinate system whose pole coincides with the axis of symmetry, as [*Backus*, 1967]

$$\boldsymbol{\sigma}_k^m(r) = \hat{r}U_k(r)Y_l^m(\theta,\phi) + V_k(r)\nabla_1 Y_l^m(\theta,\phi) - W_k(r)\hat{r}\times\nabla_1 Y_l^m(\theta,\phi) \quad (1)$$

In (1), k is the multiplet index and l is the harmonic degree of the multiplet. The $\exp(i\omega_k t)$ dependence has been omitted where ω_k is the degenerate frequency of the multiplet. The $2l+1$ singlets are indexed by the azimuthal order number m, with $-l \leqslant m \leqslant l$. The frequencies of the singlets are quadratically distributed in m [*Dahlen*, 1968]:

$$\omega_m = \omega_k(1+a+mb+m^2c) \quad (2)$$

where ω_m is the frequency of the mth singlet. The b coefficient results from the first-order effect of the Coriolis force, whereas the a and c coefficients are due to the earth's ellipticity and to second-order rotational effects. Very low frequency multiplets dominantly split by the Coriolis force (e.g., ${}_0S_2 - {}_0S_5, {}_1S_2 - {}_1S_4$) will display frequency distributions approximately linear in m. Higher-frequency multiplets dominantly sensitive to the the splitting effect of hydrostatic ellipticity (e.g., ${}_{11}S_4, {}_{10}S_2$) will be approximately parabolic in m. A table of the coefficients a, b, and c for some low-frequency multiplets can be found in the work by *Dahlen and Sailor* [1979].

Aspherical structure in the earth can destroy the quadratic distribution of the singlets characteristic of the RH model by coupling singlets within a multiplet and thereby associating more than one azimuthal order with each singlet. However, if, within observational error, a singlet distribution obeys the predicted quadratic, the splitting is said to be normal. When the RH model is not appropriate for explaining the observed splitting, the effect is termed anomalous. Using spherical harmonic stacking, *Buland et al.* [1979] reported the singlet frequencies of the normally split multiplets ${}_0S_2$ and ${}_0S_3$. The first proposed observation of anomalous splitting resulted from the work of *Chao and Gilbert* [1980], who found that the singlet frequencies of the multiplet ${}_3S_1$ did not fit the predictions of an RH model. This result depended strongly upon the poorly determined singlet frequency of ${}_3S_1^0$ and could not be regarded as conclusive. The first unambiguous observation of anomalous splitting was reported by *Masters and Gilbert* [1981], who demonstrated that the singlets of ${}_{10}S_2$ cover a frequency band which is 2.5 times greater than that produced for an RH model (Figure 1). The anomalous splitting of ${}_{10}S_2$ had previously been observed by *Dziewonski and Gilbert* [1973], but the observations were misinterpreted as two separate multiplets.

We present singlet frequency observations from 34 low harmonic degree multiplets obtained using a technique termed singlet stripping, which linearly estimates singlet resonance functions by recombining many low-frequency seismic recordings. The main result of this paper is that over a third of these multiplets appear to be anomalously split. These observations are compared to preliminary singlet frequency measurements determined by a second technique which nonlinearly estimates coefficients which are linear functionals of general aspherical structure. The singlet frequency estimates place constraints on the aspherical structure in the deep earth. The next two sections present the theoretical basis for the observational techniques that we have employed, discuss some problems inherent to these techniques, and mention how we can test if these problems are likely to vitiate the observations. A set of experiments with synthetic data is then presented in the hope of diagnosing potential trouble spots in the data analysis. A discussion of the observations themselves follows. We conclude with a series of tests to determine the accuracy of the observations and an inversion in the hope of illuminating the cause of anomalous splitting.

2. Forward Problem

We restrict attention to multiplets which can be regarded as isolated and, therefore, not significantly coupled to any other multiplet. This restriction can be lifted easily, from a theoretical point of view, but the singlets of strongly coupled multiplets are difficult to observe and beyond the scope of the present paper.

Consider first a spherically symmetric, nonrotating, elastic, isotropic, reference earth model. We use the symbol k to denote the three parameters which characterize a multiplet (i.e., radial order n, harmonic degree l, and multiplet type (toroidal or spheroidal)). The displacement field at a position $\mathbf{r}$ excited by a point source at $\mathbf{r}_0$ with moment rate tensor $\mathbf{M}$ can be written [*Gilbert and Dziewonski*, 1975]

$$\mathbf{s}(\mathbf{r},t) = \mathrm{Re}\left[\sum_k \boldsymbol{\sigma}_k^T(\mathbf{r})\mathbf{a}_k(\mathbf{r}_0)e^{i\omega_k t}\right] \quad (3)$$

where the superscript T represents the transpose of a vector and the inner product $\boldsymbol{\sigma}_k^T\mathbf{a}$ represents the sum over the $2l+1$ singlets each with complex degenerate frequency ω_k. The $2l+1$ components of the receiver vector $\boldsymbol{\sigma}_k(\mathbf{r})$ are given by (1) and the excitation vector $\mathbf{a}_k(\mathbf{r}_0)$ is composed of the $2l+1$ excitation coefficients $\mathbf{a}_k^m = -\mathbf{e}_k^{m*}:\mathbf{M}$, where $\mathbf{e}_k^{m*}$ is the complex conjugate of the strain tensor of the mth singlet evaluated at the source $(\mathbf{r}_0)$. Explicit expressions for the $\mathbf{e}_k^m$ in terms of the multiplet scalars U_k, V_k, W_k in (1) are given by *Gilbert and Dziewonski* [1975]. The effect of a small, general aspherical perturbation to the reference earth model has been treated in detail by *Woodhouse and Dahlen* [1978] and reviewed by *Woodhouse and Girnius* [1982]. We merely summarize the results here.

The displacement field corresponding to (3) for a general aspherical earth can be written as a bilinear form

$$\mathbf{s}(\mathbf{r},t) = \mathrm{Re}\left[\sum_k \boldsymbol{\sigma}_k^T(\mathbf{r})e^{i\mathbf{H}^k t}\mathbf{a}_k(\mathbf{r}_0)e^{i\omega_k t}\right] \quad (4)$$

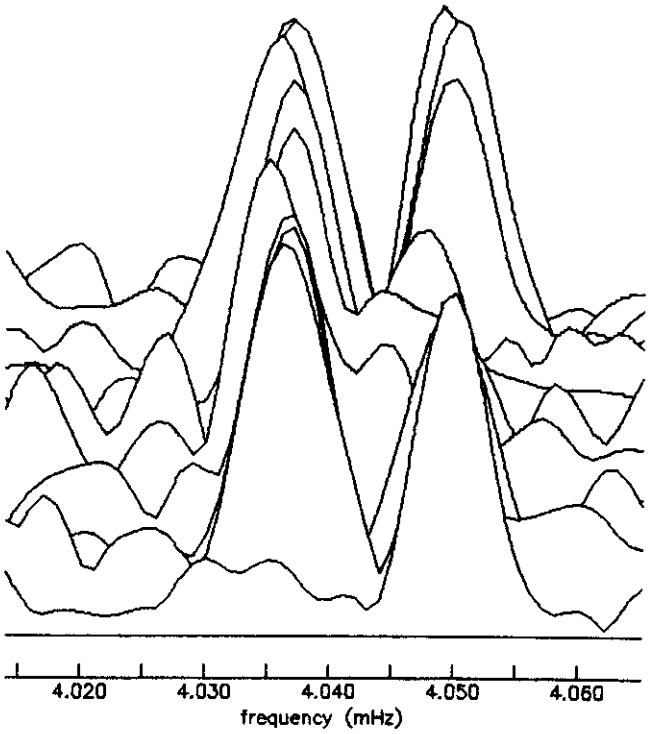

Fig. 1. Amplitude spectra of 13 recordings in the 50-μHz band around ${}_{10}S_2$ following two large, deep earthquakes (the Tonga event of 1977 and the Banda Sea event of 1982, both on June 22). The spectra are plotted as a function of absolute value of latitude so that an equatorial station would be in back and a polar station directly in front. The only spheroidal mode in this band is ${}_{10}S_2$ and can be seen to be anomalously wide, spanning more than 14 μHz though predicted to be less than 6 μHz wide for a rotating, hydrostatic earth model. The spectrum in front is for the south polar recording following the Tonga event; the single peak is consistent with the working hypothesis which forms the basis for singlet stripping (section 3).

in which the $(2l+1)\times(2l+1)$ complex splitting matrix $\mathbf{H}^k$ encodes the effect of the aspherical structure. The elements of $\mathbf{H}^k$ are linearly related to the structural perturbations which cause the splitting. For clarity we temporarily suppress the multiplet index k, then

$$H_{mm'} = \omega_k (a+mb+m^2c)\delta_{mm'} + \sum_s \gamma_s^{mm'} c_s^{m-m'} \quad (5a)$$

where

$$c_s^t = \int_0^a (\delta\kappa_s^t(r)K_s(r)+\delta\mu_s^t(r)M_s(r)+\delta\rho_s^t(r)R_s(r))r^2dr - \sum_i r_i^2 h_{si}^t B_{si} \quad (5b)$$

The first term in (5a), on the diagonal of $\mathbf{H}$, contains the splitting effects of the earth's rotation and ellipticity of figure. The second term represents the contribution by other aspherical perturbations which have been expanded in spherical harmonics with the perturbations in bulk modulus ($\delta\kappa$), in shear modulus ($\delta\mu$), in density ($\delta\rho$), and to discontinuities (h_i) at radii r_i given by

$$\delta\kappa(r,\theta,\phi) = \sum_{s,t} \delta\kappa_s^t(r) Y_s^t(\theta,\phi)$$

$$\delta\mu(r,\theta,\phi) = \sum_{s,t} \delta\mu_s^t(r) Y_s^t(\theta,\phi)$$

$$\delta\rho(r,\theta\phi) = \sum_{s,t} \delta\rho_s^t(r) Y_s^t(\theta,\phi)$$

$$h_i(\theta,\phi) = \sum_{s,t} h_{s_i}^t Y_s^t(\theta,\phi)$$

The integral kernels K_s, R_s, M_s, and B_{si} can be computed from the formulae given by *Woodhouse and Dahlen* [1978]. The $\gamma_s^{mm'}$ are real and are given by

$$\gamma_s^{mm'} = (-1)^m (2l+1)\left(\frac{2s+1}{4\pi}\right)^{1/2}\begin{pmatrix} l & l & s \\ 0 & 0 & 0\end{pmatrix}\begin{pmatrix} l & l & s \\ -m & m' & t\end{pmatrix}$$

The Wigner 3–j symbols are defined by *Edmonds* [1960] and may be easily computed using the recursion relationships summarized by *Schulten and Gordon* [1975]. The γ coefficients obey a set of selection rules and are nonzero only if s is even, $0 \leqslant s \leqslant 2l$, and $t = m - m'$. These properties limit the kind of aspherical structure to which an isolated multiplet is sensitive. For example, the first and second rules require that a multiplet of harmonic degree $l = 2$ is sensitive only to the harmonic degrees $s = 2$ and $s = 4$ of the aspherical structure.

It is conceptually and computationally useful to consider the spectral decomposition of $\mathbf{H}^k$:

$$\mathbf{H}^k\mathbf{U}^k = \mathbf{U}^k\mathbf{\Omega}^k \quad (6)$$

where $\mathbf{U}^k$ is the unitary matrix whose columns are the eigenvectors of $\mathbf{H}^k$ and $\mathbf{\Omega}^k$ is the diagonal matrix of eigenvalues. Equation (4) can then be rewritten in component form

$$\mathbf{s}(\mathbf{r},t) = \mathrm{Re}\left[\sum_k \sum_{j=1}^{2l+1} u_k^j(\mathbf{r}) b_k^j(\mathbf{r}_0) e^{i(\omega_k+\Omega_{jj}^k)t}\right] \quad (7)$$

with

$$\mathbf{u}_k(\mathbf{r}) = \sigma_k^T(\mathbf{r})\mathbf{U}^k \qquad \mathbf{b}_k(\mathbf{r}_0) = (\mathbf{U}^k)^{-1}\mathbf{a}_k(\mathbf{r}_0)$$

$\mathbf{U}_k$ rotates the receiver and excitation vectors into the normal coordinates of the perturbed earth and $\mathbf{\Omega}^k$ splits the singlet frequencies, associating the jth eigenfrequency $\omega_j = \omega_k + \Omega_{jj}^k$ with the singlet shape $\mathbf{u}_k^j(\mathbf{r})$.

A considerable simplification of (7) arises if $\mathbf{H}^k$ is diagonal. Inspection of (5) reveals that this will result if each singlet is sensitive only to rotation, ellipticity of figure, and other axisymmetric structure ($t = 0$). In this case, $\mathbf{U}^k = \mathbf{I}$, so

$$\mathbf{s}(\mathbf{r},t) = \mathrm{Re}\left[\sum_k \sum_{m=-l}^{l} \sigma_k^m(\mathbf{r}) a_k^m(\mathbf{r}_0) e^{i(\omega_k+\Omega_{mm}^k)t}\right] \quad (8)$$

and $\mathbf{H}^k = \mathbf{\Omega}^k$, where

$$\Omega_{mm} = \omega_k(a+mb+m^2c) + \sum_s \gamma_s^{mm} c_s^0 \quad (9)$$

3. Inverse Problem

The estimation of the aspherical structure coefficients, c_s^t, in (5b) leads to a linear inverse problem for the aspherical perturbations $\delta\rho_s^t(r), h_{si}^t$, etc. Unfortunately, (4) demonstrates that the coefficients are nonlinearly related to displacement so that their direct estimation is problematic. We have developed two techniques to attempt to estimate the c_s^t from the data.

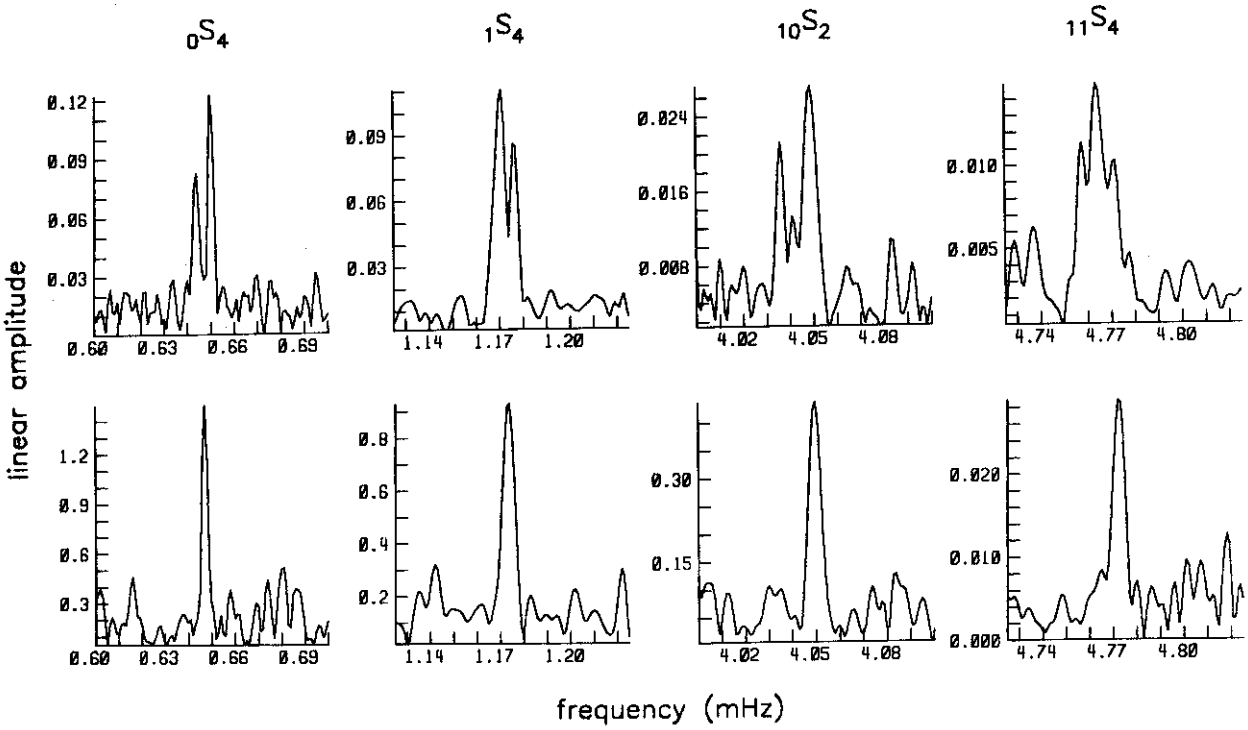

Fig. 2. Spectra of the four low harmonic degree multiplets, $_0S_4$, $_1S_4$, $_{10}S_2$, $_{11}S_4$, recorded at nonpolar (upper figures) latitudes and polar (lower figures) latitudes. Each nonpolar spectrum shows clear evidence of splitting, though the polar spectra are not obviously split. These observations are the basis for our working hypothesis that the singlet shapes of the low harmonic degree multiplets are dominantly single spherical harmonics so that $\mathbf{U}^k \approx \mathbf{I}$. Both $_{10}S_2$ and $_{11}S_4$ span a frequency band of more than 13 μHz, though predicted to be less than 7 μHz wide by the RH model. Such multiplets are termed anomalously wide. Upper spectra are (from left) HAL 1977, 231; CMO 1977, 231; NNA 1977, 173; HAL 1977, 173.

3.1. *Singlet Stripping*

If an accurate estimate of the eigenvector matrix for the kth multiplet, $\mathbf{U}^k$, is available, then we can Fourier transform (7)

$$\mathbf{s}_p(\mathbf{r},\omega) = \sum_k \sum_{j=1}^{2l+1} A_{kp}^j C_k^j(\omega) \tag{10}$$

in which p denotes a single component of a source-receiver pair, $A_{kp}^j = u_k^j(\mathbf{r}) b_k^j(\mathbf{r}_0)$, and $C_k^j(\omega)$ is the singlet resonance function—the Fourier transform of the decaying cosinusoid in the time domain. The complex excitation A_{kp}^j can be computed if the source mechanism of each earthquake is known. With many recordings from a number of events, (10) can be solved linearly to estimate the singlet resonance functions (see section 5). The complex frequencies of the singlets then can be determined from the estimated resonance functions using any one of a number of methods [e.g., *Masters and Gilbert*, 1983]. The procedure is very similar to the singlet stripping algorithm proposed by *Gilbert* [1971] and the multiplet stripping algorithm of *Gilbert and Dziewonski* [1975]. Therefore it is termed singlet stripping. If the proposed eigenvector matrix and the measured singlet frequencies are sufficiently accurate, $\mathbf{H}^k$ can be reconstructed by (6). The c_s^l can then be estimated by (5*a*).

In general, the a priori knowledge of $\mathbf{U}^k$ without a knowledge of the singlet frequencies is unlikely. One exception occurs at very low frequencies where the splitting effect of the earth's rotation is very large. For these rotationally dominated multiplets (e.g., $_0S_2$–$_0S_5$, $_1S_2$–$_1S_4$), $H_{mm'} \approx mbw_k\delta_{mm'}$ by (5*a*), so that the splitting matrix is approximately diagonal and $\mathbf{U}^k \approx \mathbf{I}$. A simple test of this observation is based on the fact that if $\mathbf{U}^k = \mathbf{I}$, then on a vertical component recording each singlet has the geographical shape of a single $Y_l^m(\theta,\phi)$ as in (1). In particular, a vertical recording at one of the geographical poles should contain only one singlet corresponding to Y_l^0. Indeed, Figure 2 shows that this is the case for $_0S_4$ and $_1S_4$, both of which are clearly split at lower latitudes. More interestingly, Figure 2 reveals that a single south polar peak is apparent for some nonrotationally dominated, high Q, low harmonic degree multiplets which are PKP or PKIKP equivalent (e.g., $_{10}S_2, _{11}S_4$). The observation of a single peak at the south pole for a number of low harmonic degree multiplets ($l \lesssim 5$) suggests that we might fruitfully adopt $\mathbf{U}^k \approx \mathbf{I}$ as a working hypothesis for these multiplets and apply singlet stripping to many low harmonic degree multiplets. We are then faced with the practical problem of determining a posteriori when the working hypothesis has been satisfied.

There are several a posteriori checks on the validity of the working hypothesis that $\mathbf{U}^k \approx \mathbf{I}$. First, since singlet stripping estimates resonance functions which are of known analytic form, failure is indicated by deviation from the appropriate form. Often this failure is visually apparent (Figure 8), but subtle cases can be resolved by attempting to fit an analytic resonance function to the estimated function in a least squares sense. A second a posteriori check is provided by (9). It is feasible to evalu-

ate the γ_s^{mm} defined in (6) explicitly from the recurrence relations of *Schulten and Gordon* [1975] for small values of harmonic degree s, e.g.,

$$\gamma_2^{mm} = \left(\frac{5}{4\pi}\right)^{1/2} \frac{1}{(2l+3)(2l-1)} [l(l+1)-3m^2] \quad (11a)$$

and

$$\gamma_4^{mm} = \frac{9}{8\sqrt{\pi}} \frac{1}{(2l+5)(2l+3)(2l-1)(2l-3)} \cdot [3l(l+1)(l+2)(l-1)+m^2(25-30l(l+1))+35m^4] \quad (11b)$$

Equation (9) then implies that if the perturbing axisymmetric structure is of harmonic degree $s=2$, the singlet frequencies will obey a quadratic in m but with the a and c coefficients augmented. If $s=4$ axisymmetric structure is also present, then the singlet frequencies will obey a quartic in m (without a cubic term). Moreover, since (11) possesses no m-linear terms, the m-linear coefficient in the best fitting polynomial should approximate the Coriolis splitting term $b\omega_k$. If an observed singlet frequency distribution departs significantly from one of these simple polynomials with the Coriolis m-linear term, it is likely that the working hypothesis has been violated and the singlet frequency estimates for the multiplet are suspect. The results from singlet stripping can then be compared with those from a different observational technique described below. Finally, the singlet frequencies satisfying these criteria can be used to estimate c_2^0 coefficients by (9), which are then subject to the test that they be consistent with a geophysically reasonable model of the aspherical structue of the earth.

3.2. *Nonlinear Parameter Estimation*

The second technique (developed and applied independently by *Woodhouse and Giardini* [1985]) is a nonlinear regression in which we linearize the dependence of displacement on the aspherical structure coefficients, c_s^t, in (4). We can then iteratively solve for small general aspherical perturbations δc_s^t from a starting model of aspherical structure. The inclusion of a perturbation to the degenerate frequency, ω_k, is also desirable since it is often not independently well known. Letting c_j be one of the c_s^t, the linearized forward problem for an isolated multiplet is

$$\mathbf{s}(\mathbf{r},t)_{\text{obs}} = \mathbf{s}(\mathbf{r},t) + \sum_j \frac{\partial \mathbf{s}(\mathbf{r},t)}{\partial c_j} \delta c_j + \frac{\partial \mathbf{s}(\mathbf{r},t)}{\partial \omega_k} \delta\omega_k \quad (12)$$

A rapid algorithm for the computation of the derivative seismograms is presented in the appendix. Equation (12) is then Fourier transformed, and the c_s^t are estimated by iteratively fitting the complex spectra of many recordings in the frequency band surrounding the multiplet(s) of interest.

In principle, this method has the advantage over singlet stripping that no a priori knowledge of aspherical structure is required. In fact, the two techniques are complementary in many ways. In practice, if the amount of structure is large, the linearization may be a poor approximation and care must be taken to determine the likelihood of convergence to a spurious mimimum in the neighborhood of the starting model. Prior estimates of the degenerate frequency and overall splitting width are also desirable in order to choose the appropriate frequency band for the spectral fitting. Fortunately, singlet stripping will often reveal the band over which a multiplet is split even when it fails to estimate accurately all of the constituent singlet frequencies. Indeed, singlet stripping has often proven effective at determining whether a multiplet is anomalously widely split (see section 5), a phenomenon which can only result from large, nonhydrostatic aspherical structure. Thus the application of singlet stripping prior to the nonlinear regression can help determine when the linearization is inappropriate as well as provide the frequency band for fitting. The results from the nonlinear regression remain difficult to evaluate quantitatively. It has been our experience that the standard minimum variance error analysis yields grossly optimistic estimates of the errors in the coefficients, and many a posteriori numerical experiments must be performed to gauge which coefficients are required to fit the data. In this paper, we use the nonlinear regression only as one test of the validity of the observations from singlet stripping. A more detailed discussion of the technique, together with its systematic application to many low-frequency multiplets, is the subject of a future contribution.

4. EFFECT OF NONAXISYMMETRIC STRUCTURE ON SINGLET STRIPPING

The remainder of this paper discusses the application of singlet stripping to a large data set under the working hypothesis that $\mathbf{U}^k \approx \mathbf{I}$. This hypothesis is only rigorously valid for an axisymmetric earth; since departures from axisymmetry are well known (e.g., continent-ocean structure), it is essential at this point to try to evaluate the effect of nonaxisymmetric structure (i.e., deviation of $\mathbf{U}^k$ from $\mathbf{I}$) on singlet stripping. We must inquire, first, how nonaxisymmetric heterogeneity will affect the observed singlet frequencies within a multiplet and, second, how it will affect the subsequent estimate of the c_2^0 coefficient and hence the axisymmetric model. In the attempt to answer these questions, we have performed a series of experiments with synthetic data in which progressively larger amounts of nonaxisymmetric structure have been included in the models which form the basis for the experiments.

The results from any experiment with synthetic data are model dependent, and the choice of realistic models is necessary to insure the value of the experiment. For ease of presentation we restrict attention to models representing degree 2 structure alone. The following results have proven not to be changed significantly by the inclusion of higher-order structure. We base our experiments on hybrids of the degree 2 part of the lower mantle model (L02.56) of *Dziewonski* [1984] and the upper mantle model (M84A) of *Woodhouse and Dziewonski* [1984]. These authors have chosen to represent their models as perturbations in v_p and v_s^2, respectively. We require the coefficients c_2^t given by (5*b*) and therefore perturbations in κ, μ, and ρ. We follow *Anderson et al.* [1968] and *Masters et al.* [1982] and use the following scaling relationships:

$$\frac{d\ln v_p}{d\ln v_s} = 0.8 \quad \frac{d\ln\rho}{d\ln v_s} = 0.4$$
$$\frac{d\ln\kappa}{d\ln\rho} = 3.5 \quad \frac{d\ln\mu}{d\ln\rho} = 6.0 \tag{13}$$

At this point a little nomenclature is helpful. We call this whole mantle degree 2 model DW2. We then define model p as the RH model added to p times DW2, so that model 0 is the RH model, model 2 is the RH model plus twice DW2, and so on. In general, as p increases, the model becomes less axisymmetric. We now review the results for three different types of multiplets: a well-split rotationally dominated multiplet (${}_1S_4$), a well-split PKP equivalent multiplet almost entirely insensitive to the Coriolis force (${}_{11}S_4$), and a poorly split mantle multiplet weakly sensitive to the Coriolis force (${}_2S_4$). Since we desire realistic models and since model 1 does not accurately predict the splitting widths of ${}_{11}S_4$ and ${}_2S_4$, we supplement the c_2^0 coefficients for these multiplets to match their observed splitting widths.

4.1. *Effect on the Estimated Singlet Frequencies*

Figures 3*a* and 3*b* present the results from the synthetic experiment for the rotationally dominated multiplet ${}_1S_4$. Each row in both figures represents a different model, with model 0 (the RH model) on top and progressively less axisymmetric models lower in the figure. For model 0, the c_2^0 coefficient is zero indicating that no supplement to the c_2^0 coefficient is needed to match the splitting width of ${}_1S_4$. The modulus of the complex eigenvector matrix $\mathbf{U}^k$ is symbolically represented in the first column of Figure 3*a* by boxes whose sizes are directly proportional to the magnitudes of the matrix elements. Matrix elements range in size from zero to 1.0; boxes for elements less than 0.1 in magnitude have not been plotted, and those for elements greater than 0.9 are solid. For comparison, the modulus of the eigenvector matrix for model 3 has been included in Table 1. The nonaxisymmetric models all possess nonzero c_2^t coefficients and, as one moves down the figure, $\mathbf{U}^k$ progressively diverges from $\mathbf{I}$, indicating the divergence from the working hypothesis. All the structure coefficients used to construct the synthetic data in these experiments are presented in Table 2. The amplitude spectrum of the synthetic seismogram for each model is plotted for a south pole receiver in the second column. Only a single peak appears for the RH model, but more than one peak clearly is apparent for model 5. (Recall that in section 3 the observation of a single south polar peak in the real data was used as evidence for the potential success of singlet stripping.) The first column of Figure 3*b* contains the amplitude spectra of the resonance functions estimated by singlet stripping applied to 30 noise-free synthetic seismograms from five events. They are plotted in the narrow frequency band surrounding ${}_1S_4$ such that the singlet for which $m=-l$ lies in back and the one for which $m=+l$ lies in front. The singlet frequencies estimated from these resonance functions are plotted in the second column of Figure 3*b* together with the average 1σ errors estimated from the experiment with real data (see Figure 9*a* and Table 4 in section 5). The c_2^0 coefficient is estimated using (9) and the m-quadratic then given by (9) is plotted as the solid curve. The estimated c_2^0 coefficients themselves are plotted in Figure 6 and are discussed below. The input frequencies are also plotted for comparison. The analogous plots from the experiment with real data are shown in Figures 8*a* and 8*e*.

The results for ${}_1S_4$ are not particularly surprising. Inspection of Figure 3*b* shows that due to the dominance of the Coriolis force, even models with unrealistically large amounts of nonaxisymmetric heterogeneity (e.g., model 5) yield reasonably accurate singlet frequency measurements. For model 5, eight of the nine estimated singlet frequencies are within 1σ of the input values even though estimated resonance functions are clearly contaminated by spurious peaks. Thus singlet stripping applied to rotationally dominated multiplets appears quite robust. The observation of a single south polar peak in the real data (Figure 2) places constraints on the amount of nonaxisymmetric heterogeneity affecting ${}_1S_4$. Since the polar peak for model 5 in Figure 3*a* already shows signs of degradation due to coupling between the singlets, a realistic simulation of the real data is given by model 3.

Figures 4*a* and 4*b* contain the results of the synthetic experiment for ${}_{11}S_4$. The c_2^0 coefficient for model 0 is nonzero in this case since it has been chosen to be large enough to fit the overall splitting width of the multiplet. The estimated resonance functions in Figure 4*b* show signs of degradation for model 1, and many multiple peaks are apparent for model 2. Again, however, the majority of the singlet frequency measurements are accurate; seven of the nine singlet frequencies are within 1σ of the input values for model 2. The south polar peak exhibits a shoulder structure for model 1.5, although multiple peaks are not observed until model 2. Model 1.5 probably provides the best simulation of the experiment with real data found in Figures 9*d* and 9*h*.

Things are not as straightforward for the weakly split multiplet ${}_2S_4$ as shown in Figures 5*a* and 5*b*. The evaluation of the results is complicated by the added problem of poor spectral resolution; nine resonance functions are packed into $6\,\mu$Hz rather than the $14\,\mu$Hz of ${}_{11}S_4$ or the $18\,\mu$Hz of ${}_1S_4$. Even for model 3 in Figure 5*b*, most of the estimated resonance functions appear to be nearly singletlike, although many of the singlet frequency measurements are clearly in error. Furthermore, only a single peak is apparent on all the polar records in Figure 5*a*, though unlike the single peaks in the synthetic experiments for ${}_{11}S_4$ or ${}_1S_4$ (or the real data for ${}_2S_4$) the polar peaks for models 2 and 3 have center frequencies significantly different from the frequency estimated for the $m=0$ singlet by singlet stripping. Also, unlike model 3,

Fig. 3*a*. (opposite) Results from the synthetic experiment for ${}_1S_4$. The four rows represent models 0, 1, 3, and 5, with the models lower in the figure possessing more nonaxisymmetric structure. (See Table 2 for the c_2^t for each model.) In the left column are moduli of the complex eigenvector matrices $\mathbf{U}$ for each model, represented by boxes whose sizes are proportional to the magnitudes of the matrix elements. Matrix elements range in size from 0.0 to 1.0; boxes with magnitudes <0.1 are open and >0.9 are solid. Model 0 is the RH model for which $\mathbf{U}=\mathbf{I}$. The addition of nonaxisymmetric heterogeneity causes $\mathbf{U}$ to diverge from $\mathbf{I}$. The right column possesses the synthetic south pole spectrum for each model. Multiple peaks conflict with real observations such as those in Figure 2.

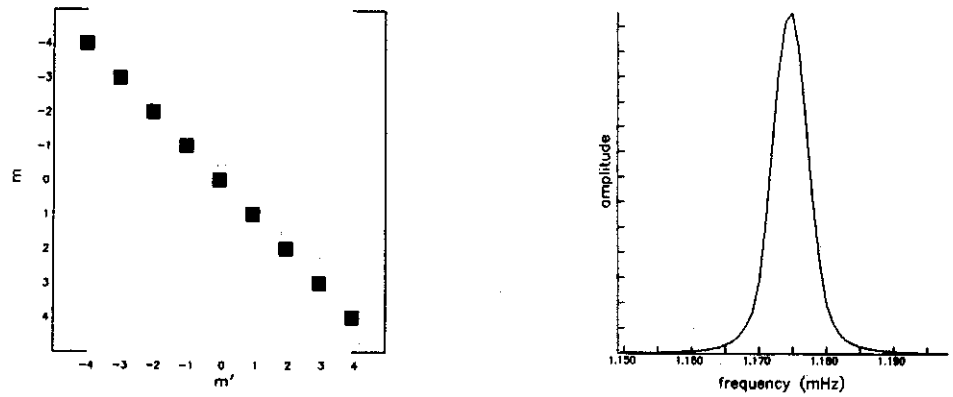
m
m'
amplitude
frequency (mHz)

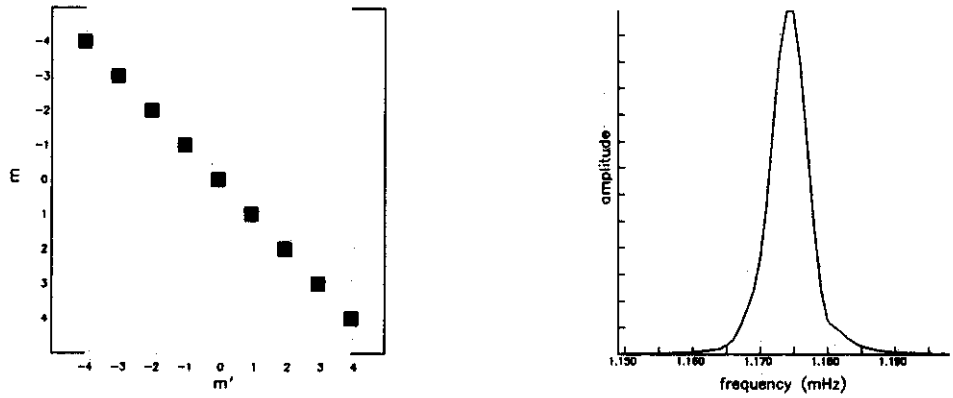
m
m'
amplitude
frequency (mHz)

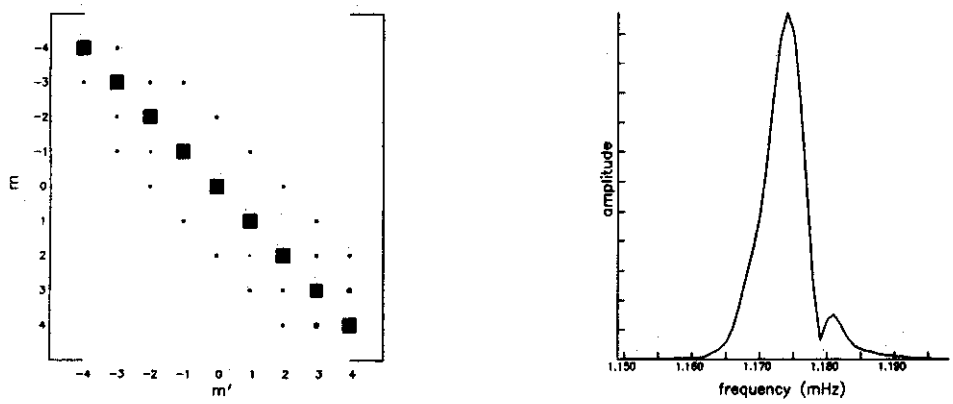
m
m'
amplitude
frequency (mHz)

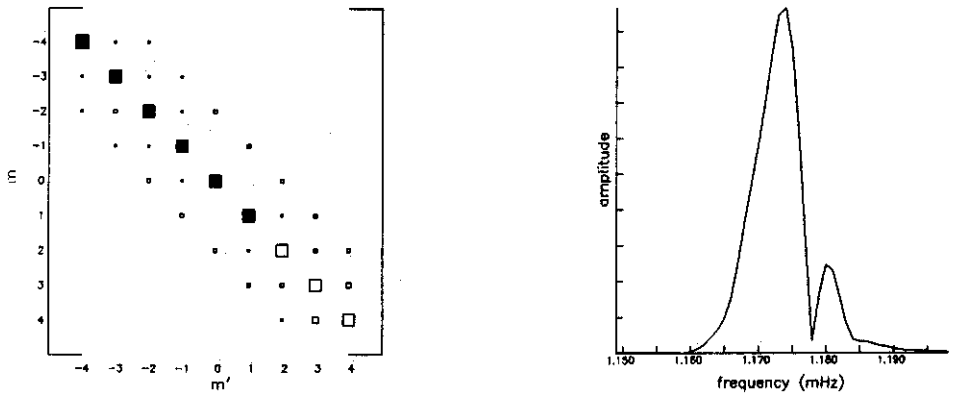
m
m'
amplitude
frequency (mHz)

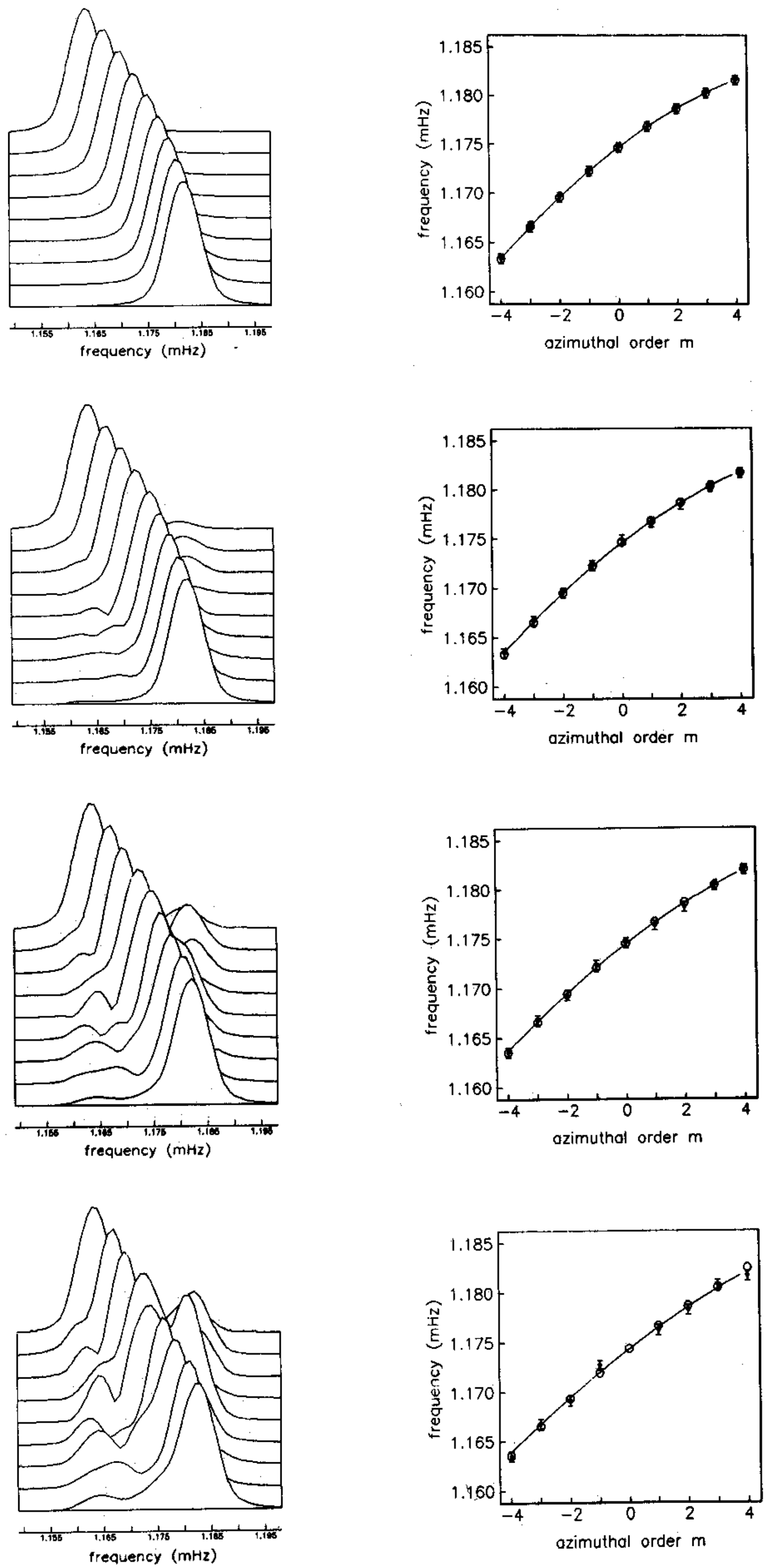
1.155
1.165
1.175
1.185
1.195
frequency (mHz)
1.185
1.180
1.175
1.170
1.165
1.160
frequency (mHz)
-4
-2
0
2
4
azimuthal order m

TABLE 1. Modulus of Eigenvector Matrix for $_1S_4$, Model 3

					m'				
	0.99	0.11	0.07	0.01	0.01	0.00	0.00	0.00	0.00
	0.12	0.98	0.11	0.12	0.01	0.01	0.00	0.00	0.00
	0.07	0.13	0.98	0.09	0.15	0.01	0.01	0.00	0.00
	0.01	0.11	0.11	0.97	0.05	0.17	0.01	0.02	0.00
m	0.00	0.01	0.14	0.06	0.97	0.04	0.17	0.02	0.14
	0.00	0.01	0.01	0.17	0.03	0.97	0.09	0.17	0.04
	0.00	0.00	0.01	0.00	0.18	0.10	0.95	0.17	0.14
	0.00	0.00	0.00	0.01	0.01	0.16	0.20	0.93	0.25
	0.00	0.00	0.00	0.00	0.01	0.02	0.11	0.27	0.96

Compare with Figure 3*a*, model 3.

the real data (Figure 9*b* and 9*f*) with one exception possess singlet frequency estimates which fit the m-quadratic quite well. Thus model 2 probably provides a conservative simulation of the real data: a single peak at the south pole with approximately the same frequency as the estimated $m = 0$ frequency and frequencies which fit the quadratic at the 2σ level. Thus, for weakly split multiplets the errors estimated for the singlet frequencies might be slightly optimistic. This is to be expected because the error analysis that we use [*Dahlen*, 1982] assumes that the only source of error is random Gaussian noise. If an estimated resonance function is actually composed of two (or more) singlets, the singlet frequency estimate will be biased in a nonrandom way. Dahlen's error analysis easily generalizes to multiple peaks, but for poorly split multiplets like $_2S_4$ the existence of a second peak is often hard to diagnose. In practice, we will supplement the errors for $_2S_4$ and other weakly split multiplets, but we should bear in mind that the problem of spectral resolution is at least potentially serious for weakly split multiplets.

4.2. *Effect on the Estimated c_2^0 Coefficients*

In most cases, singlet stripping appears to be quite robust, yielding accurate singlet frequency measurements in the presence of relatively large amounts of nonaxisymmetric heterogeneity. The second consideration is whether the frequencies can then be used to invert for axisymmetric heterogeneity through the estimation of the c_2^0 coefficient for each multiplet. The concern here is with what statisticians call specification error [*Johnston*, 1984], which refers to any error in specifying the variables to be included in a regression. In general, an underspecification (e.g., fitting a line to a quadratic) results in biased estimates of the specified coefficients. In general, the size of the bias must be determined empirically.

In the present application, due to the working hypothesis that $\mathbf{U}^k \approx \mathbf{I}$, the specification of the relationship between the axisymmetric structure coefficient c_2^0 and the singlet frequency perturbations given by (9) necessarily does not include the contribution of nonaxisymmetric structure. The fact that the above synthetic experiments show the working hypothesis to be good enough to estimate accurate singlet frequencies even in the presence of significant nonaxisymmetric coefficients is not evidence that the c_2^0 estimates will be unbiased. We can attempt to estimate the bias in the c_2^0 coefficients by using the results of the synthetic experiments above. Figure 6 contains the estimated c_2^0 coefficients and associated 1σ errors, plotted for the models found in Figures 3–5. The input c_2^0 coefficients are also plotted for comparison. Figure 6*a* shows that a c_2^0 coefficient accurate to within 1σ will be found for $_1S_4$ even for model 5 which probably possesses an unrealistically large amount of nonaxisymmetric structure. For the more realistic model 3, the c_2^0 estimate is unbiased at the 1σ level and statistically indistinguishable from zero, consistent with the result with real data (see Table 4 in section 5). However, Figures 6*b* and 6*c* demonstrate that as nonaxisymmetric heterogeneity increases for $_{11}S_4$ and $_2S_4$, the c_2^0 estimate tends to be biased high. Since the nonaxisymmetric heterogeneity in the models used in these experiments acts to increase the splitting width of these multiplets, it effectively aliases into the c_2^0 estimate, increasing its magnitude. A conservative estimate of the bias in c_2^0 might be put at the 2σ level. It should be mentioned that this bias is only in the c_2^0 estimate and does not jeopardize the observation of the anomalous width of multiplets which rests on the more accurate singlet frequency observations themselves.

In conclusion, although care must be taken not to be misled by narrowly split multiplets, singlet stripping appears to be quite robust, yielding accurate singlet frequency estimates in the presence of realistic amounts of nonaxisymmetric structure. The use of these frequencies to invert directly for axisymmetric heterogeneity is underspecified and therefore complicated by nonaxisymmetric structure biasing the estimated c_2^0 coefficients. For this reason, in the present paper we have restricted the inverse problem for axisymmetric heterogeneity to be a check on the geophysical reasonableness of the estimated

TABLE 2. Structure Coefficients (μHz) Used to Construct Synthetic Data in Section 4

	c_2^0	$\mathrm{Re}c_2^1$	$\mathrm{Im}c_2^1$	$\mathrm{Re}c_2^2$	$\mathrm{Im}c_2^2$
$_1S_4$					
Model 0	0.00	0.00	0.00	0.00	0.00
Model 1	−0.36	0.61	−0.19	−0.09	1.30
Model 3	−1.08	1.81	−0.56	−0.26	3.90
Model 5	−1.80	3.03	−0.94	−0.44	6.50
$_{11}S_4$					
Model 0	13.70	0.00	0.00	0.00	0.00
Model 1	13.70	2.40	0.68	0.03	5.80
Model 1.5	13.70	3.59	1.08	0.05	8.70
Model 2	13.70	4.79	1.37	0.07	11.60
$_2S_4$					
Model 0	7.70	0.00	0.00	0.00	0.00
Model 1	7.70	0.86	0.00	−0.68	1.88
Model 2	7.70	1.71	0.00	−1.37	3.76
Model 3	7.70	2.57	0.00	−2.05	5.65

Values are in microhertz.

Fig. 3*b*. (opposite) Results from the synthetic experiment for $_1S_4$ (continued). Each row corresponds to the same model as in Figure 3*a*. In the left column are the resonance functions estimated by singlet stripping applied to 30 noise free synthetic seismograms for each model. (See Figure 8 caption for plot format description.) Multiple peaks are apparent for model 5. In the right column are comparisons between the singlet frequencies estimated from the resonance functions (triangles with 1σ errors) and the input singlet frequencies (octagons). The best fitting m-quadratic polynomial given by the c_2^0 coefficient estimated from the singlet frequencies (9) is plotted as the solid line. Good agreement between estimated and input frequencies holds even for model 5.

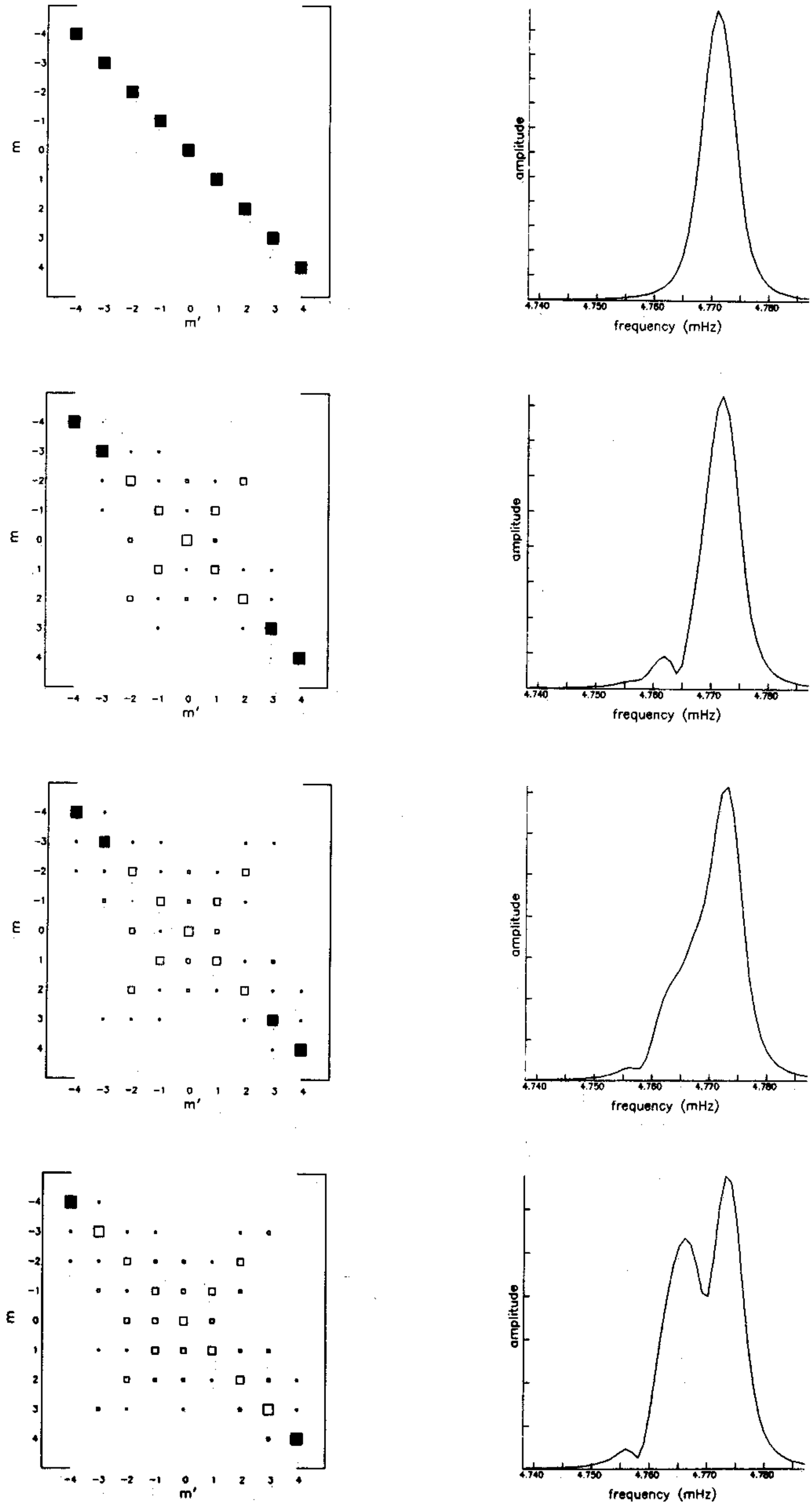
m
-4 -3 -2 -1 0 1 2 3 4
m′
-4 -3 -2 -1 0 1 2 3 4
amplitude
frequency (mHz)
4.740 4.750 4.760 4.770 4.780
m
m′
amplitude
frequency (mHz)
m
m′
amplitude
frequency (mHz)
m
m′
amplitude
frequency (mHz)

c_2^0 coefficients and to explore the nature of anomalous splitting. This will be discussed further in section 6. In section 5 we present the observational results from singlet stripping applied to the real data and conclude with a series of checks on the estimated singlet frequencies.

5. APPLICATION OF SINGLET STRIPPING

Equation (10) forms the basis for the data analysis, and when our working hypothesis is valid, we have

$$\mathbf{s}_p(\omega) = \sum_k \sum_{m=-l}^{l} A_{kp}^m C_k^m(\omega) \tag{14}$$

where m is the azimuthal order number of the singlet. In general, A_{kp} has a slight dependence on frequency in the vicinity of a multiplet if the moment rate tensor has a finite time duration or spatial extent. At the low frequencies considered in this work we find that the moment rate tensor can be adequately represented by

$$\mathbf{M}(t) = \mathbf{M}_0 g(t) \tag{15}$$

where $g(t)$, the source time function, is assumed to be triangular. For large earthquakes this term introduces a phase delay into the seismograms which is essential to model the data. The exact form of $g(t)$ is not important, and the observed phase shift can be accommodated by using the source centroid time [*Dziewonski et al.*, 1981]. Source parameters used in the present work are given in Table 3. The resulting frequency dependence of a_k^m is very weak and, if we consider small frequency bands about the multiplets of interest, we can neglect it. Given many source receiver pairs, (14) can be regarded as a matrix equation which can be solved to evaluate the C_k^m at a discrete set of frequencies. Writing the solution in terms of the generalized inverse of $\mathbf{A}$,

$$\hat{C}_k^m(\omega) = \sum_p (A_{kp}^m)^{-1} s_p(\omega) \tag{16}$$

A good algorithm for performing the operation (16) is the SVD algorithm for multiple right-hand sides of *Golub and Reinsch* [1971]. In the experiments we describe below, we use approximately 200 recordings so the matrix $\mathbf{A}$ will typically be only 400× 20 real numbers, and the SVD can be readily handled by a microcomputer.

The complex frequencies of the singlets are determined from their estimated resonance functions using the (least squares) algorithm described by *Masters and Gilbert* [1983] and errors are assigned using the analysis of *Dahlen* [1982]. Related methods are those of *Bolt and Brillinger* [1979] and *Hansen* [1982]. Imaginary part frequencies (i.e., Q values) display too much scatter within all multiplets to be of value in constraining aspherical anelastic structure. However, real part frequencies are quite stable and have been compared with those obtained by the autoregressive method [*Chao and Gilbert*, 1980] and the moment ratio method [*Buland and Gilbert*, 1978] with differences never exceeding the observational error.

The practical application of singlet stripping is complicated by the fact that our data are not perfect and the matrix $\mathbf{A}$ may be in error. The long time series required to investigate low-frequency, high-Q multiplets are often contaminated by aftershocks, noise bursts, and data gaps. These are usually treated by zeroing the offending time periods of bad data, giving a panel structure to the time series. The spectrum modification caused by panel structure can be severe if gaps are large. This is due to the convolution of the broad spectrum of the panel structure with the spectrum of the uncontaminated time series. In principle, this can be handled by explicitly including the convolution in $\mathbf{A}$, thus making the matrix $\mathbf{A}$ frequency dependent and very large. In practice, records with large gaps must be discarded.

Another problem is that the data must be corrected for instrument response. The success of source mechanism estimation at low frequencies from both International Deployment of Accelerometers (IDA) and Global Digital Seismic Network (GDSN) data suggests that the instrument phase responses are quite well known. However, we have experienced considerable difficulty with the very long period Seismic Research Observatory (SRO) and Abbreviated SRO (ASRO) amplitude response which can be wrong by as much as a factor of 2 (R. Woodward and G. Masters, unpublished manuscript, 1986). Noise levels also vary considerably among records, and the naive implementation of the singlet stripping technique yields very poor results. The best results are produced by weighting the pth record with

$$w_p = \bar{s}_p^{-1}(1-\bar{s}_p/s_{\max})$$

where $\bar{s}_p$ and $s_{\max}$ are the mean and peak values, respectively, of the amplitude spectrum of the pth record in a small frequency band surrounding the target multiplet. As well as penalizing noisy records and rewarding peaky records, this weighting scheme effectively corrects for instrument amplitude miscalibration. The improvement we get by weighting is demonstrated in Figure 7 where we show the amplitude spectrum of the estimated resonance functions of two singlets of ${}_1S_4$ retrieved with and without the weighting scheme discussed above. All the data series are Hanning tapered in the time domain to suppress spectral leakage so the resulting resonance functions implicitly include the effect of the taper. (The algorithm for estimating the complex frequencies from the resonance functions also incorporates the effect of the taper.)

From a practical point of view, the most difficult aspect of singlet stripping is the judgement of the quality of the results. Figure 8*a* shows the amplitude spectra of the nine estimated resonance functions of ${}_1S_4$ obtained by applying the singlet stripping algorithm to 190 IDA and GDSN recordings from five large events. We have no difficulty in assessing the results because the individual resonance functions are narrow and reasonably well separated in frequency. Furthermore, all the resonance functions can be well fit by a synthetic resonance function, and the singlet frequencies are well fit by the quadratic in m, see (9), which is produced by the estimated c_2^0 coefficient (Figure 8*e*). The results are consistent with our working

Fig. 4*a*. (opposite) Results from the synthetic experiment for ${}_{11}S_4$. (See Figure 3*a* caption for plot format description.) The four rows represent models 0, 1, 1.5, and 2. Due to insensitivity to the Coriolis force, the diagonality of $\mathbf{U}$ breaks down much more rapidly as nonaxisymmetric structure is added, than for ${}_1S_4$. Multiple peaks are observed on the south pole synthetic for model 2.

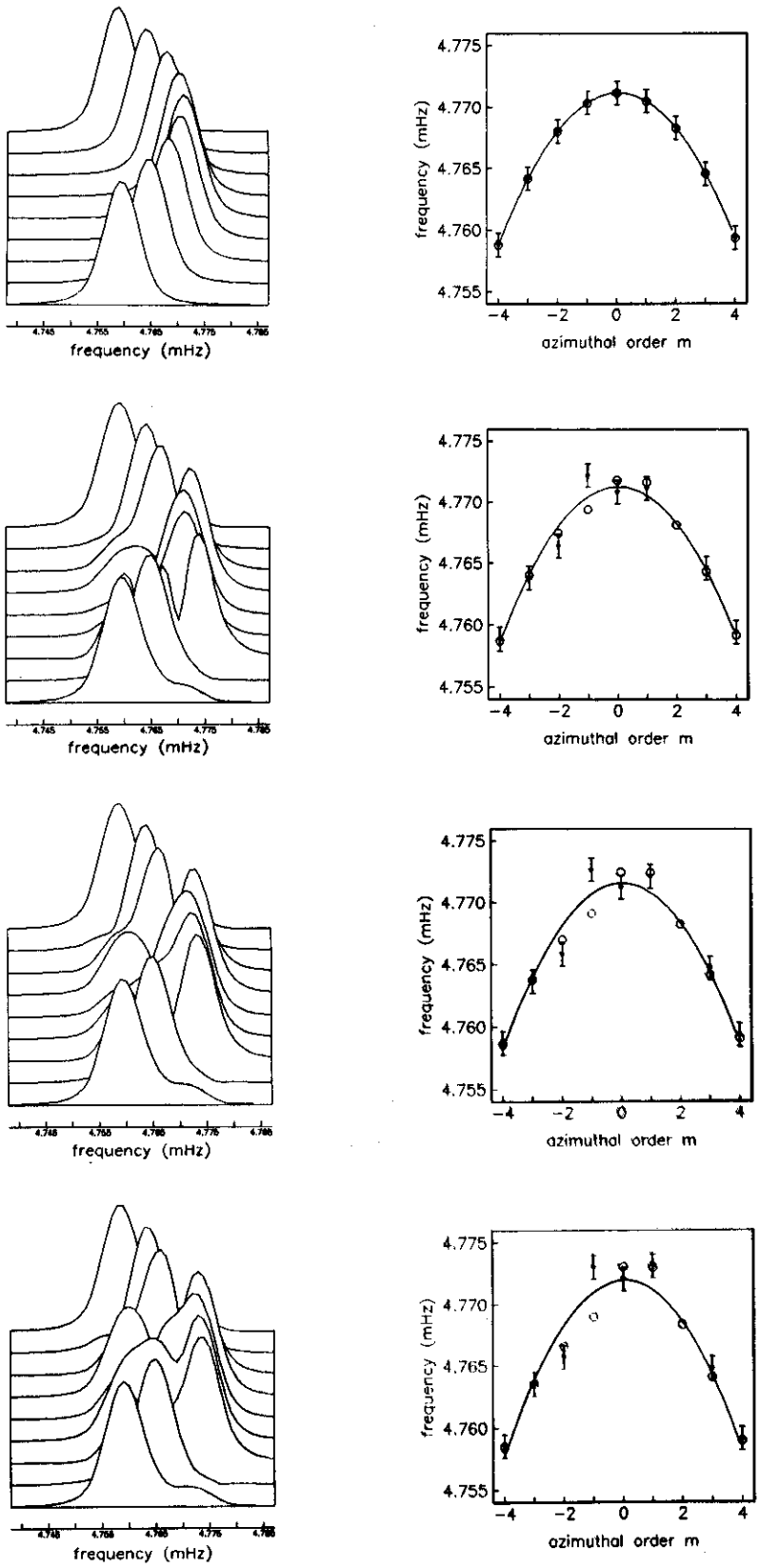

Fig. 4*b*. Results from the synthetic experiment for ${}_{11}S_4$ (continued) (See Figure 3*b* caption for plot format description.) Each row corresponds to the same model as in Figure 4*a*. The resonance functions estimated for model 1 shows signs of degradation, though most singlet frequency estimates are accurate even for model 2.

hypothesis that $\mathbf{U} \approx \mathbf{I}$, which is not surprising in view of the theoretical dominance of Coriolis splitting for ${}_1S_4$ and the results of the synthetic experiments in section 4. If the individual resonance functions were so broad that the total splitting width of the multiplet was less than the width of a single resonance function, we would be unable to assess whether we had reliably isolated individual singlets. Due to this practical consideration of spectral resolution, we have restricted attention to multiplets for which we can minimize peak widths by taking long records without significantly degrading the spectra with noise [*Dahlen*, 1982]. This restricts us to the high-Q and/or low-frequency multiplets.

The restriction to low harmonic degree, high-Q multiplets limits us to 50 candidate multiplets of which we have at least partially resolved 34. The observations of these 34 multiplets fall naturally into two categories: (1) the normally split multiplets whose singlet frequencies closely follow the predictions of an RH model and (2) the anomalously split multiplets for which singlet stripping gives apparently reasonable results. Figures 8*a*–8*d* contain the amplitude spectra of the estimated resonance functions of five normally split multiplets (${}_1S_4$, ${}_0S_4$, ${}_1S_3$, ${}_3S_1$, ${}_5S_5$) plotted in the narrow frequency band surrounding each, so that the singlet for which $m = -l$ lies in back and the one for which $m = l$ lies in front. (We jointly recovered the resonance functions of ${}_1S_3$ and ${}_3S_1$ and have plotted them together in Figure 8*c* with ${}_1S_3$ in front of ${}_3S_1$.) To illustrate the normality of the splitting pattern, the estimated resonant frequencies are plotted versus azimuthal order m in Figures 8*e*–8*h*, together with the estimated 1σ errors associated with each singlet. Equation (9) and the observed singlet frequencies can be used to estimate ω_k, c_2^0, and their associated errors for each multiplet. The estimated m-quadratic given by (9) is plotted as a solid line in Figures 8*e*–8*h*, and the dashed line is the quadratic predicted for the RH model (2). For the sake of comparison, the predicted degenerate frequency has been equated to the estimated degenerate frequency. The observations fit the predictions quite well; in fact, all the estimated c_2^0 coefficients are statistically indistinguishable from 0 at the 2σ level. All estimates of degenerate frequencies and c_2^0 coefficients (where appropriate), together with 1σ errors, are included in Table 4.

For brevity, singlet frequency observations have not been tabulated. However, for most multiplets the frequency distribution generated by a c_2^0 estimate matches the observed frequencies within observational error. One can calculate the frequencies predicted by a c_2^0 coefficient by taking it and the degenerate frequency observation from Table 4 and using (11*a*), (9), and the fact that $\omega_m = \omega_k + \Omega_{mm}$. *Dahlen and Sailor* [1979] tabulate splitting parameters (a, b, and c) for all the multiplets considered here with $n < 4$. Our Table 5 contains splitting parameters for the remainder of the multiplets. The authors will gladly supply the observed singlet frequencies upon request.

Although the splitting characteristics of many multiplets agree well with the predictions for the RH model, many others are anomalously split. The observation of anomalous splitting is not completely dependent on the employment of a multiple record technique such as the one described here. Indeed, some multiplets can be observed to be anomalously split on individual records. Figure 1 contains 12 amplitude spectra of the multiplet ${}_{10}S_2$ following two large deep events: the large Tonga event of 1977 and the Banda Sea event of 1982, both on June 22. The total splitting width of this multiplet can be seen to be approximately 14 μHz, whereas the predicted width for an RH model is less than 6 μHz. Multiplets like ${}_{10}S_2$ and ${}_{11}S_4$ (Figure 2) which span frequency bands much broader than predicted for an RH model are termed anomalously wide. It is not uncommon for an anomalously split multiplet to be anomalously wide, and we frequently find it useful to characterize the results by the ratio R of the observed to predicted splitting widths. (R values are included in Table 4.) No anomalously narrow multiplets have been unambiguously observed. About a third of the multiplets are anomalously wide with $R > 1.3$. We have discussed in section 4 how the imperfect resolution of individual singlets can make the determination of the distribution of singlets difficult. The splitting width, however, is entirely insensitive to problems associated with the misidentification of singlets within a multiplet. The R value is a highly robust datum and an R value significantly greater than unity provides a compelling argument for the existence of large departures of the earth from the RH model.

Figure 9 contains diagrams similar to those in Figure 8, but for anomalously split multiplets (${}_0S_6$, ${}_2S_4$, ${}_6S_3$, ${}_{11}S_4$). ${}_0S_6$ is an example of a multiplet whose estimated singlet distribution differs greatly from the predictions of an RH model, but with a comparable splitting width. The remaining multiplets in Figure 9 are anomalously wide with splitting width ratios $R > 1.5$ (see Table 4). All the anomalously widely split multiplets are SKS, PKP, or PKIKP equivalent multiplets, which are greatly sensitive to aspherical structure in the lower mantle and core. The singlet distributions of all four of the multiplets in Figure 9 also fit quadratics in m well, although now a quadratic different from that predicted for an RH model. In fact, only two multiplets are significantly nonquadratic in the distribution of their singlets (${}_{10}S_2$ and ${}_{13}S_2$). The estimated resonance functions and singlet frequencies of ${}_{13}S_2$ are plotted in Figure 10. The singlets for $m = \pm 1$ of ${}_{13}S_2$ are about 4 μHz lower in frequency than that given by the best fitting quadratic. Nevertheless, the near equality of the $m = \pm 1$ singlet frequencies means that the singlet distribution of ${}_{13}S_2$ is still well fit by a simple m-polynomial, this being an m-quartic without the m-cubic and, due to the insensitivity to the Coriolis force, m-linear terms.

6. Evaluation and Modeling of the Observational Results

The application of singlet stripping to many low-l, high-Q multiplets appears to have allowed us to resolve more than 290 singlets from 34 multiplets. Although most of the multiplets appear to be normally split, approximately a third are anomalously wide, requiring us to postulate the existence of large, deep nonhydrostatic aspherical structure. In the present section we will further consider the accuracy of the singlet frequency measurements,

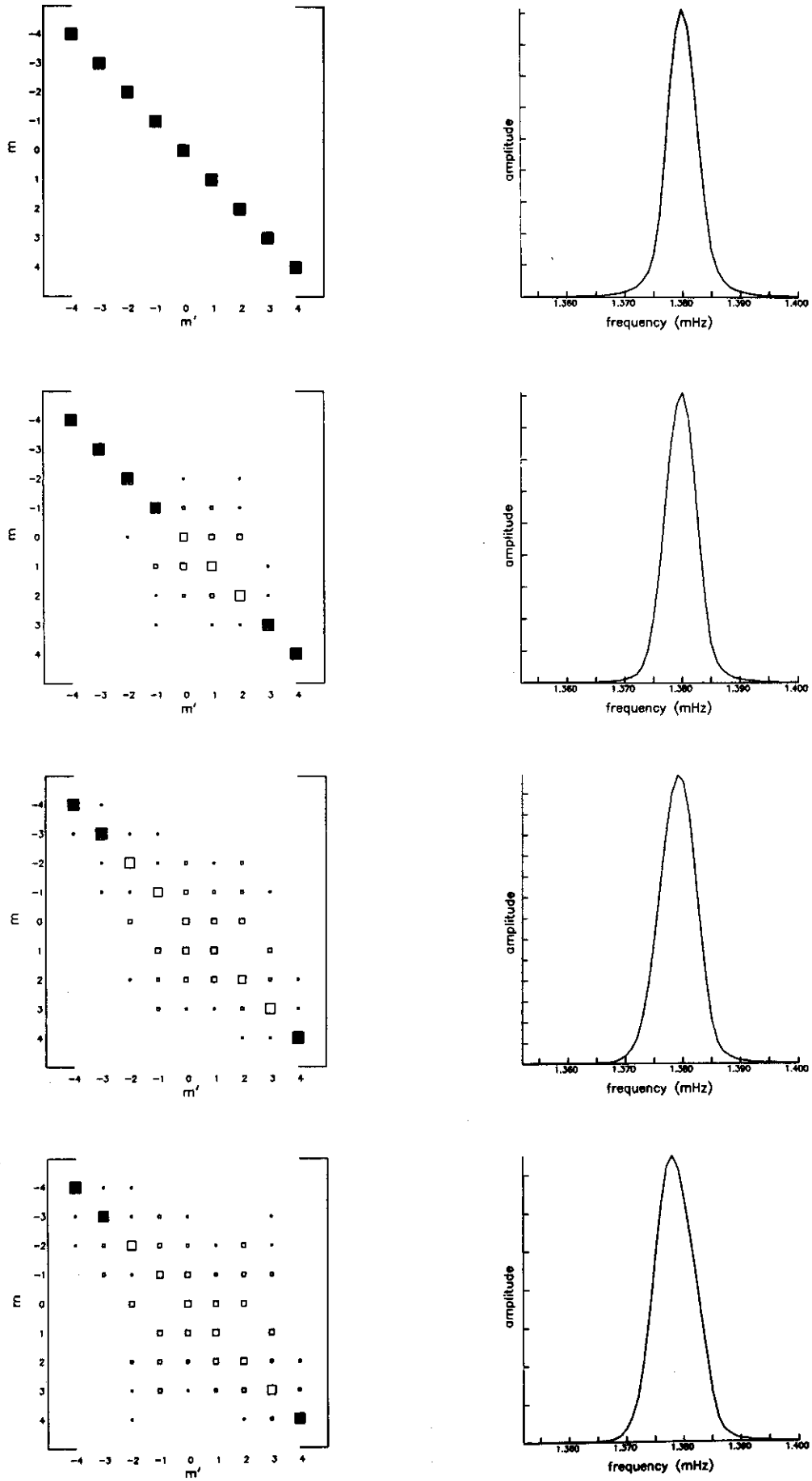
m
m'
amplitude
frequency (mHz)
1.360
1.370
1.380
1.390
1.400

by performing a comparison with preliminary results acquired from the nonlinear regression (12). We will then consider the internal consistency of the c_2^q estimates and the cause of anomalous splitting, by inverting for axisymmetric structure.

Since singlet stripping is based on a working hypothesis of unknown validity prior to its application, a series of tests must be performed a posteriori to gauge the accuracy of the observations. We have argued that the singlet frequencies constituting a multiplet should be accepted only if they approximate a low-order polynomial in azimuthal order m. We have further argued that the singlet frequency of an estimated resonance function should be accepted only if the resonance function has the appropriate analytic form. This has been insured by least squares fitting an analytic resonance function [*Masters and Gilbert*, 1983] with the misfit incorporated in the error of the singlet frequency [*Dahlen*, 1982]. The experiments with synthetic data reported in section 4 (for ${}_2S_4$) indicate, however, that these two criteria may be insufficient to diagnose failure: when singlets are closely spaced, erroneous singlet frequencies and errors can result from the presence of unidentified resonance functions. For this reason, a further test is desirable, and we present a comparison of a subset of the stripping results to preliminary results from the nonlinear regression. A more exhaustive comparison will be included in a future contribution.

Figure 11 contains the singlet frequencies and 1σ errors estimated by singlet stripping (triangles), together with the frequencies determined from the c_2^q estimated by the nonlinear regression (octagons) for the normally split multiplets ${}_1S_4$ (Figure 11*a*) and ${}_5S_5$ (Figure 11*b*), and the anomalously split multiplet ${}_{13}S_2$ (Figure 11*c*). The frequencies are represented as perturbations to the frequencies predicted for an RH model and are plotted versus azimuthal order m. Thus a value of zero for a given singlet implies agreement with the RH model. Figures 11*a* and 11*b* show that with a few exceptions, the two techniques agree within 1σ for both ${}_1S_4$ and ${}_5S_5$. The agreement is not as good for ${}_{13}S_2$ (Figure 11*c*), with the very large discrepancy for the $m=+1$ singlet resulting from the fact that the singlet frequency distribution observed by singlet stripping cannot be fit by $s=2$ structure alone. Thus either the $m=+1$ frequency estimated by singlet stripping is wrong (which is not improbable given the likelihood of strong coupling between the $m=\pm 1$ lines), or $s=4$ structure greatly affects ${}_{13}S_2$ (which appears likely since a relatively large c_4^q coefficient is estimated by the nonlinear regression). In either case, however, both techniques agree that the c_2^q coefficient is very large for ${}_{13}S_2$ and that the multiplet is anomalously widely split.

The moduli of the complex eigenvector matrices estimated by the nonlinear regression for ${}_1S_4$, ${}_5S_5$, and ${}_{13}S_2$ are represented in Figure 12. Figure 12*b* shows that the eigenvector matrix for ${}_5S_5$ is far different from the identity matrix, even though the singlet frequencies estimated by singlet stripping and the nonlinear regression are in good agreement. Moreover, the seismic wave forms for many of the multiplets considered here can only be accurately modeled by the inclusion of nonaxisymmetric heterogeneity (Figure 13). These facts are consistent with the conclusion reached from experiments with synthetic data in section 4. Indeed, a comparison of the nonlinear regression with singlet stripping indicates that singlet stripping is quite robust, yielding accurate singlet frequencies in the presence of significant amounts of nonaxisymmetric structure. Unfortunately, also in agreement with the synthetic experiments, many of the c_2^q coefficients may be biased. Figure 14 shows the c_2^q coefficients and errors estimated by singlet stripping (triangles) plotted with the estimates from the nonlinear regression (octagons) along the fundamental mode branch between ${}_0S_3$ and ${}_0S_9$. Agreement is generally good, except for ${}_0S_6$ for which the coefficient estimated from singlet stripping is probably biased high.

The results of this comparison of techniques and the synthetic experiments of section 4 suggest that the potential bias in the estimated c_2^q coefficients will generally be between one and two standard deviations. Many of the estimated c_2^q coefficients in Table 4 are significantly different from zero at greater than the five standard deviation level. It is therefore of interest to inquire if we can find an axisymmetric aspherical structure which will fit these observations. From singlet stripping we have estimated 34 c_2^q coefficients. The coefficients for ${}_0S_8$ and ${}_0S_9$ are not used in the inversion since these multiplets are known to be coupled to nearby toroidal multiplets [*Masters et al.*, 1983]. We also do not use the coefficient estimated for ${}_3S_2$, since it appears to be inconsistent with the remainder of the data set and is probably biased by a poorly determined $m=0$ singlet frequency. This restricts us to a set of 31 c_2^q coefficients. Equation (5*b*) forms the basis for the linear inversion for aspherical structure. We rewrite this for $s=2$, $t=0$ as

$$c_{2k}^q = \int_0^a G_2^k(r)\delta m_2^q(r)r^2dr - \sum_d h_{2d}^q B_{2d}^k r_d^2 \quad (17a)$$

where k is the multiplet index and where

$$G_2^k(r) = K_2^k(r)\kappa(r)\left(\frac{\partial \ln\kappa}{\partial \ln\rho}\right) + M_2^k(r)\mu(r)\left(\frac{\partial \ln\mu}{\partial \ln\rho}\right) + R_2^k(r)\rho(r) \quad (17b)$$

and

$$\delta m_2^q(r) = \delta\rho_2^q(r)/\rho(r) \quad (17c)$$

The scaling relationships (13) used in the synthetic experiments of section 4 to avoid unphysical, anticorrelated perturbations in κ, μ, and ρ are also used in (17*b*) and are similar to the implicit scalings used when computing the splitting effect of hydrostatic ellipticity. The model con-

Fig. 5*a*. (opposite) Results from the synthetic experiment for ${}_2S_4$. (See Figure 3*a* caption for plot format description.) The four rows represent models 0, 1, 2, and 3. Like ${}_{11}S_4$, the eigenvector matrix diverges rapidly from I as nonaxisymmetric heterogeneity is added. Due to poor resolution between the singlet, no double peaks are observed on the south pole synthetics. However, the single peaks for models 2 and 3 are shifted to frequencies lower than the peaks for models 0 and 1 and the frequency estimated for the $m=0$ singlet. Like the observation of multiple peaks on the south pole recording, this is diagnostic of the effect of nonaxisymmetric structure.

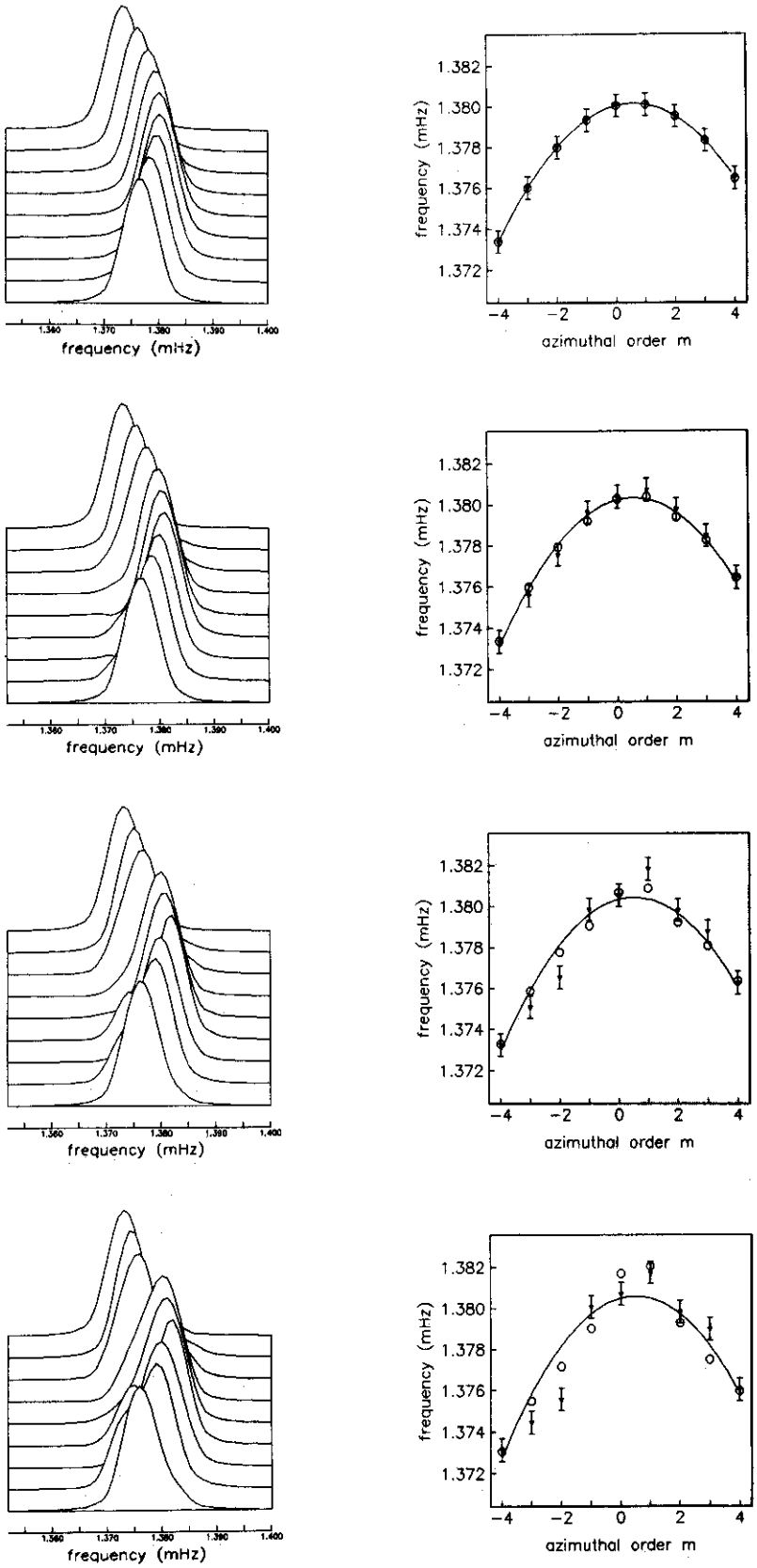

Fig. 5*b*. Results from the synthetic experiment for ${}_2S_4$ (continued). (See Figure 3*b* for plot format description.) Each row corresponds to the same model as in Figure 5*a*. Poor resolution causes the estimated resonance functions, which are clearly in error for model 3, to look singlet like. Frequencies estimated are then erroneous. In practice, frequency error estimates for poorly split multiplets will be augmented, but this problem is, at least potentially, serious for narrowly split multiplets.

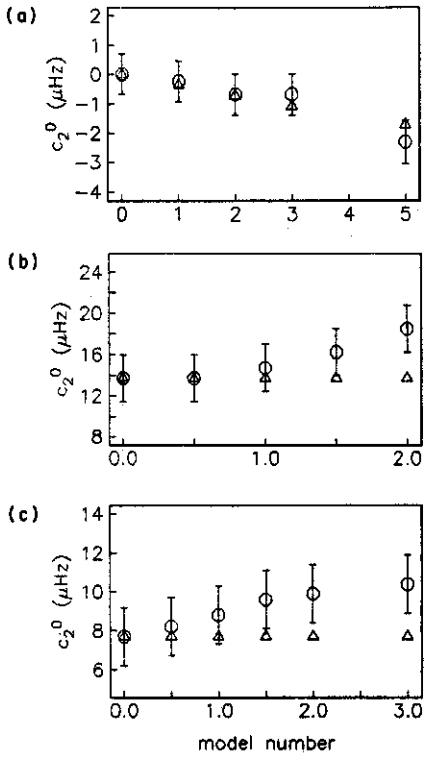

Fig. 6. The c_2^0 estimates from the synthetic experiment obtained by singlet stripping (octagons with 1σ errors) compared to the input values for each model (triangles), for (*a*) ${}_1S_4$, (*b*) ${}_{11}S_4$, and (*c*) ${}_2S_4$. Estimates are all within 1σ of input values for ${}_1S_4$ but show biasing high for ${}_{11}S_4$ and ${}_2S_4$. This is a general property of underspecified regressions.

structed (17*c*) will be expressed as a density perturbation relative to the SNREI earth model 1066A of *Gilbert and Dziewonski* [1975]. This perturbation is in addition to the earth's ellipticity of figure.

We follow *Gilbert et al.* [1973] and minimize the 2-norm radial second derivative of the model and thereby construct radially smooth models. In an attempt to produce physically reasonable models, we impose the following constraints during inversion. First, we constrain the models to match other data: the degree 2 axisymmetric part of the geoid corrected for hydrostatic effects [*Nakigoblu*, 1982] and the peak shifting patterns for ${}_0S_{20} - {}_0S_{35}$ of *Masters et al.* [1982]. Second, we apply bounds on the discontinuity jumps, and finally, we require the outer core to be in hydrostatic equilibrium (unpublished manuscript, D. Stevenson, 1986). Model 1066A contains four first-order discontinuities: inner core boundary (ICB), core mantle boundary (CMB), Moho, and free surface. The free surface and the Moho are constrained to fit the observed flattening of the earth and the $s=2$ axisymmetric part of the ocean-continent pattern, respectively. The aspherical perturbations to the CMB and ICB are allowed to fluctuate by 10 km. Since the addition of axisymmetric $s=4$ structure does not improve the fit to the data, we only report on $s=2$ models here. We consider initially models with nonhydrostatic structure only in the mantle and call the model so constructed the hydrostatic core model, for reasons soon to become apparent.

Define χ^2 goodness of fit as

$$\chi^2 = \sum_k (c_k - c_k^p)^2/\sigma_k^2$$

where $\hat{c}_k$ is the estimated coefficient with standard deviation σ_k and c_k^p is the coefficient predicted for the multiplet k for the constructed model. The RH model has a χ^2 of 580 which is reduced to 195 by the hydrostatic core model shown in Figure 15, a variance reduction of 66%. Unfortunately, this model systematically misfits the most strongly split multiplets. For example, the splitting width of ${}_{11}S_4$ is under predicted (Figure 16, dashed line). The model attempts to fit these multipets by putting oscillatory, large amplitude structure in the upper mantle. A consequence of this is that the c_2^0 coefficients for some of the multiplets sensitive to upper mantle structure are not well predicted. We have found that this sytematic misfitting can be alleviated simply by removing the constraint that the core be in hydrostatic equilibrium. The resulting model (Figure 15, dashed line) has a χ^2 of 125 corresponding to an overall variance reduction of 78%. In particular, the SKS, PKIKP, and PKP equivalent multiplets such as ${}_{11}S_4$ are now reasonably well fit (Figure 16, solid line). This nonhydrostatic core model could be regarded as a reasonable fit to the data if the bias in the c_2^0 coefficients is roughly at the two standard deviation level. (Goodness of fit statistics are summarized in Table 6.)

The result that the SKS, PKP, and PKIKP multiplets can be fit better by allowing structure in the outer core should not be surprising. These multiplets have oscillatory eigenfunctions in the mantle and are most sensitive to structure in the outer core. To illustrate this point, we present two graphs of elastic energy density versus radius. In Figure 17*a* we present the energy density of ${}_5S_5$, a nearly normally split P equivalent multiplet sensitive to

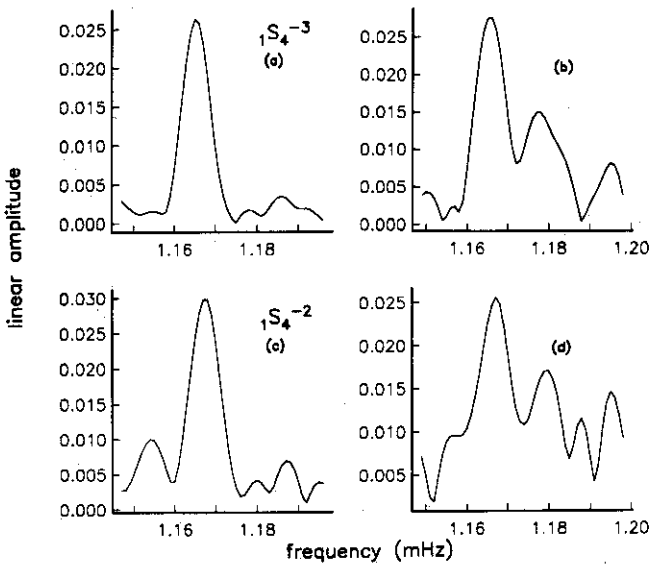

Fig. 7. Estimated singlet resonance functions for ${}_1S_4^{-3}$ (*a*) with and (*b*) without weights and for ${}_1S_4^{-2}$ (*c*) with and (*d*) without weights. Only IDA data were used in the construction of Figures *b* and *d* since mixing instrument types completely destroys the singlet strips if weights are not used. Instrument miscalibration appears to be the explanation for this.

TABLE 3. Event Specification

Event	Origin Time Year	Date	Time	Colatitude, deg	Longitude, deg	Depth, km	Number of Recordings IDA	SRO/ASRO	Total
1	1977	173	1208:33	112.88	184.10	65	7	21	28
2	1977	231	0608:55	101.09	118.46	20	7	21	28
3	1979	346	0759:03	88.40	280.64	25	10	30	40
4	1980	199	1942:23	102.53	165.92	33	8	43	51
5	1982	173	0418:40	97.34	126.04	450	13	30	43
							45	145	190

Event	Total Moment	Moment Tensor Elements M_{rr}	$M_{\theta\theta}$	$M_{\phi\phi}$	$M_{r\theta}$	$M_{r\phi}$	$M_{\theta\phi}$	Source Time*, s
1	14.10	−7.05	0.47	6.58	3.16	11.80	1.76	47
2	26.50	−26.48	23.57	2.91	0.20	−0.62	8.31	30
3	10.00	9.85	−1.15	−8.70	0.59	1.63	−3.17	50
4	7.00	6.55	−0.08	−6.47	1.80	0.28	2.01	17
5	1.40	−0.90	−0.08	0.98	0.59	0.17	0.66	5

*Half-baseline width of the source time function $g(t)$ in (15).
Moment tensor elements are in units of 10^{20} N-m.

mantle structure. In Figure 17*b* we present the energy density of ${}_{11}S_5$, an anomalously widely split PKP-equivalent multiplet with a classical turning point and a strong compressional energy concentration in the outer core. All of the anomalously widely split multiplets have significant compressional energy densities in the outer core. It may eventually prove to be possible to fit them with structure in the mantle, but this structure will be larger in amplitude and more oscillatory than the simple structure in the core.

From a seismological point of view the model with nonhydrostatic structure in the outer core seems reasonable, yet, according to Stevenson (unpublished manuscript, 1986), the amplitude perturbation of 0.4% that we infer is at least two orders of magnitude larger than currently thought possible. It is unlikely that the presence of large nonaxisymmetric structure in the mantle could explain the anomalous splitting widths of the SKS, PKIKP, and PKP equivalent multiplets. Any such nonaxisymmetric structure would have to be highly oscillatory and of large amplitude and likely to be as geophysically unacceptable as the nonhydrostatic core structure. Inversions have also shown that the existence of inner core structure can help explain some of the anomalous multiplets (e.g., ${}_{10}S_2$, ${}_{13}S_2$, ${}_{13}S_3$); however, without outer core structure a number of multiplets (e.g., ${}_{11}S_4$ and ${}_{11}S_5$) remain difficult to fit. Therefore we have a dilemma. On the one hand, the anomalously split multiplets are all primarily sensitive to structure in the core and a number of

TABLE 4. Observations of Multiplet Degenerate Frequencies ω_k, Splitting Width Ratios R, and Degree 2 Axisymmetric Structure Coefficients c_2^0

Mode	ω_k, mHz	s.d., μHz	R*	c_2^0†, μHz	s.d., μHz
${}_0S_2$	0.30961	0.15	1.0	−0.30	0.65
${}_0S_3$	0.46863	0.15	1.0	1.00	1.00
${}_0S_4$‡	0.64658	0.10	1.0	1.50	0.80
${}_0S_5$‡	0.83999	0.10	1.0	1.30	0.70
${}_0S_6$‡	1.03751	0.10	1.2	1.90	1.00
${}_0S_7$‡	1.23093	0.15	1.2	1.40	0.75
${}_0S_8$	1.41287	0.15	1.0	−0.05	0.80
${}_0S_9$	1.57752	0.15	1.0	0.60	0.70
${}_1S_2$	0.68011	0.25	1.0	−0.15	1.50
${}_1S_3$	0.93981	0.25	1.0	1.30	1.25
${}_1S_4$‡	1.17273	0.15	1.0	0.38	0.90
${}_1S_5$	1.37066	0.35	1.0	3.20	1.90
${}_1S_6$	1.52116	0.30	1.1	−2.20	2.10
${}_1S_7$	1.65522	0.25	1.1	7.50	1.55
${}_1S_8$	1.79897	0.40	1.3	14.10	2.50
${}_2S_3$	1.24343	0.20	1.7	11.20	1.30
${}_2S_4$	1.37974	0.15	1.5	3.90	0.90
${}_2S_5$	1.51578	0.25	1.3	0.65	1.45
${}_2S_6$	1.68113	0.20	1.1	−0.75	1.10
${}_3S_1$	0.94427	0.20	1.0	0.01	1.50
${}_3S_2$	1.10598	0.40	1.8	19.30	3.00
${}_4S_3$	2.04821	0.35	1.0	−0.10	2.50
${}_4S_4$	2.27963	0.45	1.7	11.70	2.50
${}_5S_3$	2.16883	0.35	1.2	3.70	2.00
${}_5S_4$	2.37864	0.30	1.2	−0.50	2.10
${}_5S_5$‡	2.70358	0.30	1.2	0.55	2.00
${}_5S_6$	3.01203	0.45	1.4	7.80	2.65
${}_6S_3$	2.82171	0.35	2.4	17.70	2.90
${}_8S_1$	2.87284	0.15	1.2	1.80	1.30
${}_{10}S_2$‡	4.04100	0.60	2.5	20.80	3.00
${}_{11}S_4$	4.76597	0.35	2.1	21.40	2.30
${}_{11}S_5$	5.07232	0.35	1.7	13.60	2.30
${}_{13}S_2$‡	4.84397	0.50	2.3	22.30	2.80
${}_{13}S_3$	5.19406	0.35	1.9	17.40	1.70

* A multiplet is anomalously wide if $R > 1.3$.
† A multiplet is anomalously split if $|c_2^0| > 2\sigma_{c_2^0}$.
‡ Nonlinear regression used to estimate c_2^0.

TABLE 5. Splitting Parameters Not Contained in Work by *Dahlen and Sailor* [1979]

Mode	a	b	c
${}_4S_3$	0.65705	0.43078	−0.16403
${}_4S_4$	0.62974	0.24861	−0.09443
${}_5S_3$	0.59788	0.34686	−0.14894
${}_5S_4$	0.64045	0.27237	−0.09621
${}_5S_5$	0.63596	0.24102	−0.06402
${}_5S_6$	0.63598	0.20838	−0.04588
${}_6S_3$	0.54846	−0.04989	−0.13550
${}_8S_1$	0.89324	0.08100	−1.33201
${}_{10}S_2$	0.59407	0.06294	−0.29584
${}_{11}S_4$	0.58659	0.01335	−0.08773
${}_{11}S_5$	0.58481	0.00523	−0.05832
${}_{13}S_2$	0.65884	0.03061	−0.32854
${}_{13}S_3$	0.60887	0.02566	−0.15186

Values are in microhertz.

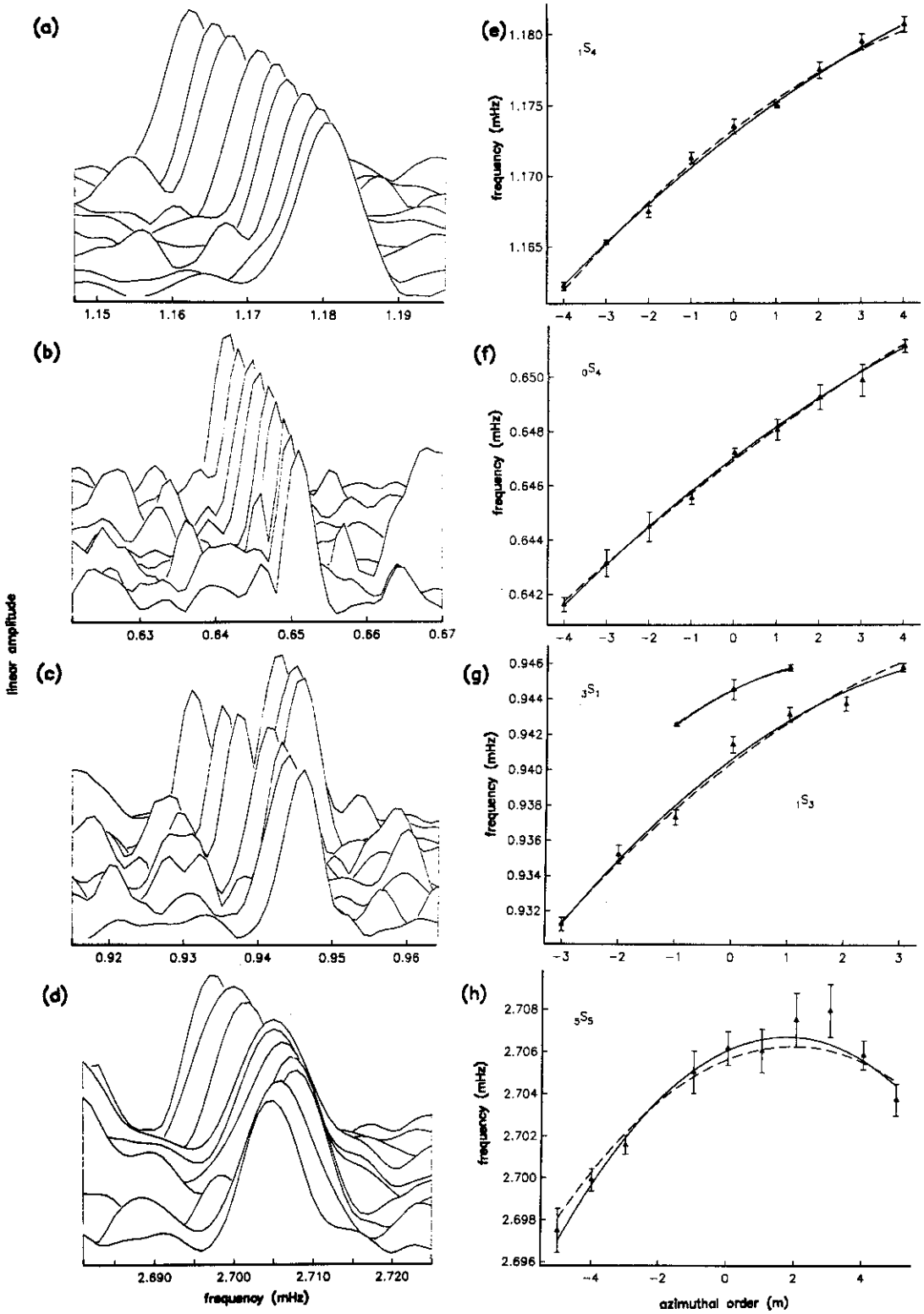

Fig. 8. Amplitude spectra of the estimated resonance functions and singlet frequencies of five normally split multiplets: *(a)–(d)* estimated resonance functions of $_1S_4$, $_0S_4$, $_1S_3$–$_3S_1$, and $_5S_5$ plotted in the narrow frequency band surrounding each, with the $m=-l$ singlet in back and the $m+l$ singlet in front. The resonance functions of $_1S_3$ and $_3S_1$ were jointly recovered and plotted together in Figure 8*c* with $_1S_3$ in front of $_3S_1$. *(e)–(h)* Singlet frequencies and 1σ errors are plotted versus azimuthal order m adjacent to the corresponding resonance function. The best fitting m-quadratic (solid curve, equation (9)) computed with estimated c_2^0 coefficient and the predicted quadratic for an RH model (dashed curve, equation (2)) are plotted such that both curves possess the same degenerate frequency.

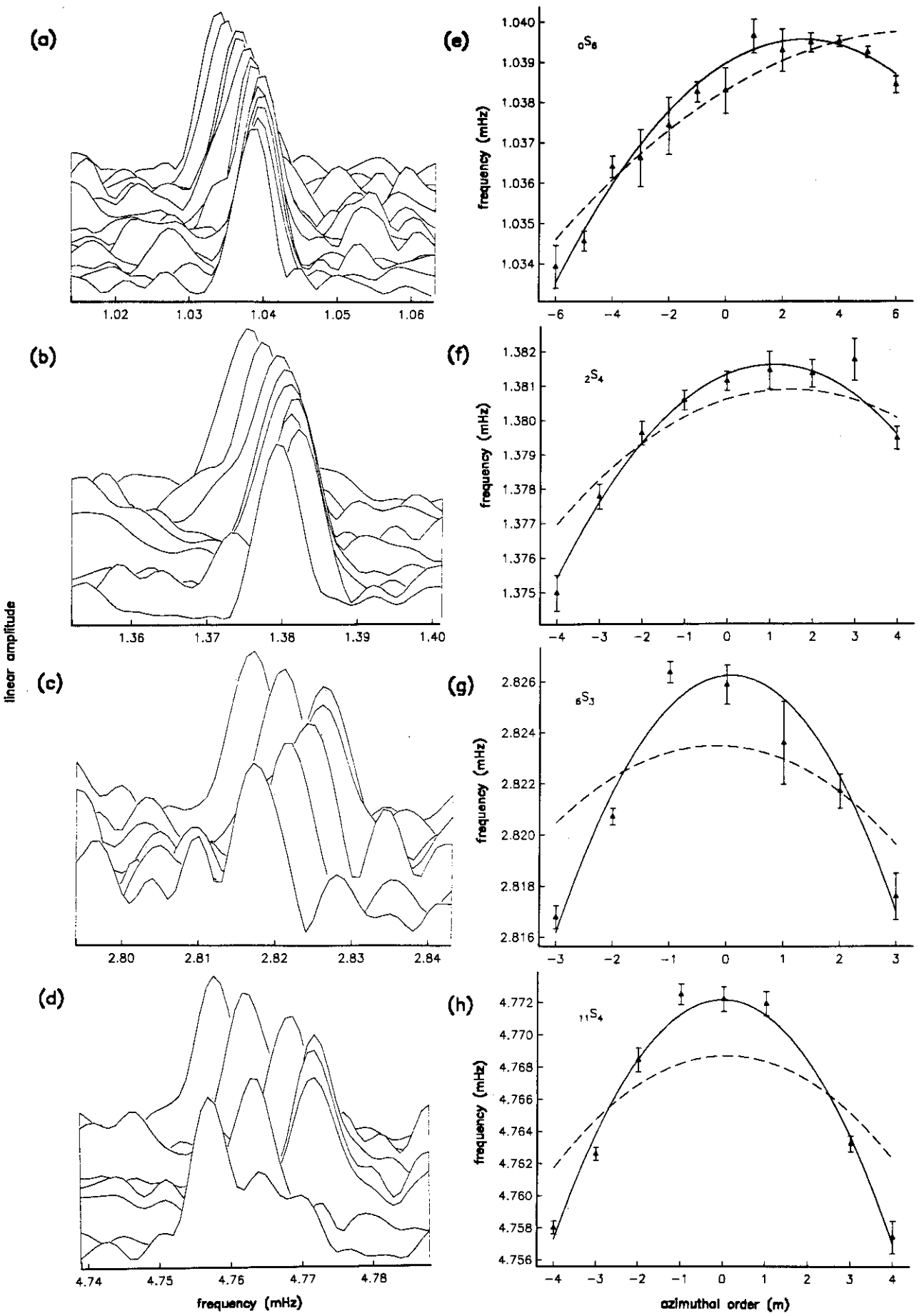

Fig. 9. Spectra and frequency plots as in Figure 8, but for the anomalously split multiplets $_0S_6$, $_2S_4$, $_6S_3$, and $_{11}S_4$. The multiplets $_2S_4$, $_6S_3$, and $_{11}S_4$ clearly can be seen to be anomalously wide.

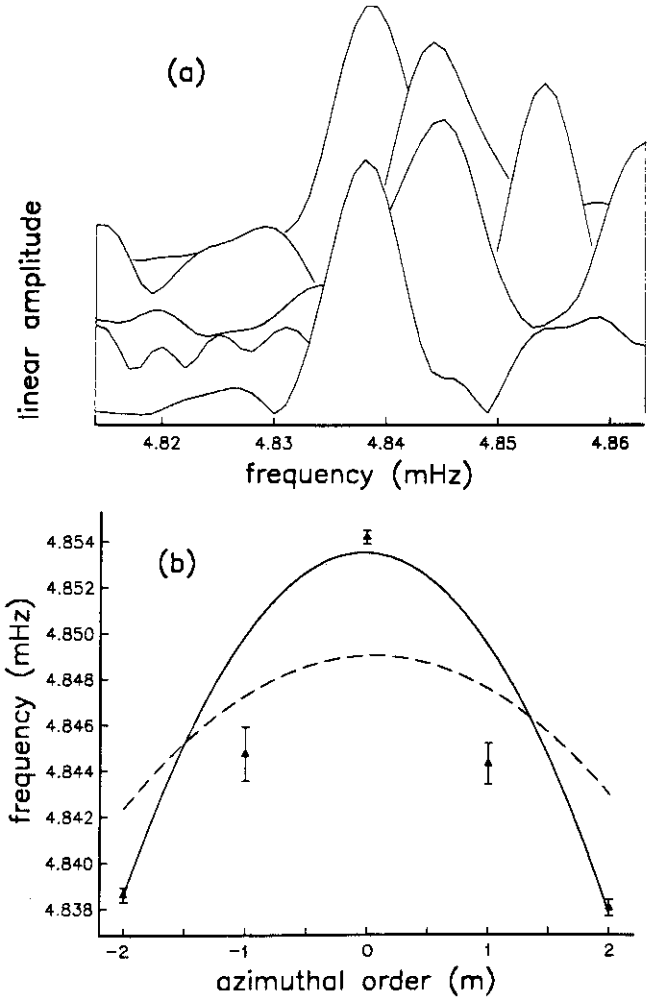

Fig. 10. (*a*) Amplitude spectra of the estimated resonance functions and (*b*) singlet frequency plots of the anomalously wide, nonquadratically split multiplet ${}_{13}S_2$. (See Figure 8 caption for general plot description.) Though nonquadratic in the distribution of its singlets, the near equality of the $\pm m$ singlets of ${}_{13}S_2$ implies that the distribution can be fit by a quartic in m (minus the cubic term) which is consistent with a sensitivity to dominantly axisymmetric heterogeneity.

multiplets are primarily sensitive to outer core structure. Thus unconstrained inversions will preferentially put the structure in the outer core. On the other hand, it is physically unrealistic for the core to be able to sustain large nonhydrostatic structure if it is compositionally homogeneous. The location and nature of the core structure needs much further investigation before it can be resolved and is the subject of a more complete discussion in a future contribution.

We note that if large-amplitude structure does exist in the core, it should be visible in the travel time residuals of core phases. *Creager and Jordan* [1986] have recently reported a strong latitude dependence of the travel time residuals of $P'_{AB}-P$ and have confirmed the latitude dependence seen in $P'_{DF}-P$ originally reported by *Poupinet et al.* [1983]. The size of the travel time difference that they observe (2 s between polar and equatorial paths) is not inconsistent with the size of structure in the nonhydrostatic core model. Polar paths are analogous to zonal harmonics ($m=0$) and equatorial paths to sectoral harmonics ($m=\pm l$). Fast polar paths imply shorter-period (higher frequency) $m=0$ lines and slow equatorial paths imply longer-period (lower frequency) $m=\pm l$ lines, in qualitative agreement with the observed splitting. Also, the residual splitting widths, after removal of the effect of the RH model, is about 2×10^{-3} of the degenerate frequencies of the anomalously widely split multiplets, a signal comparable in size to the 2-s travel time anomaly.

A characteristic common to both the hydrostatic and nonhydrostatic core models is the large (~0.8% peak) structure in the lower mantle. This structure is not theoretically unreasonable and is more than 5 times larger

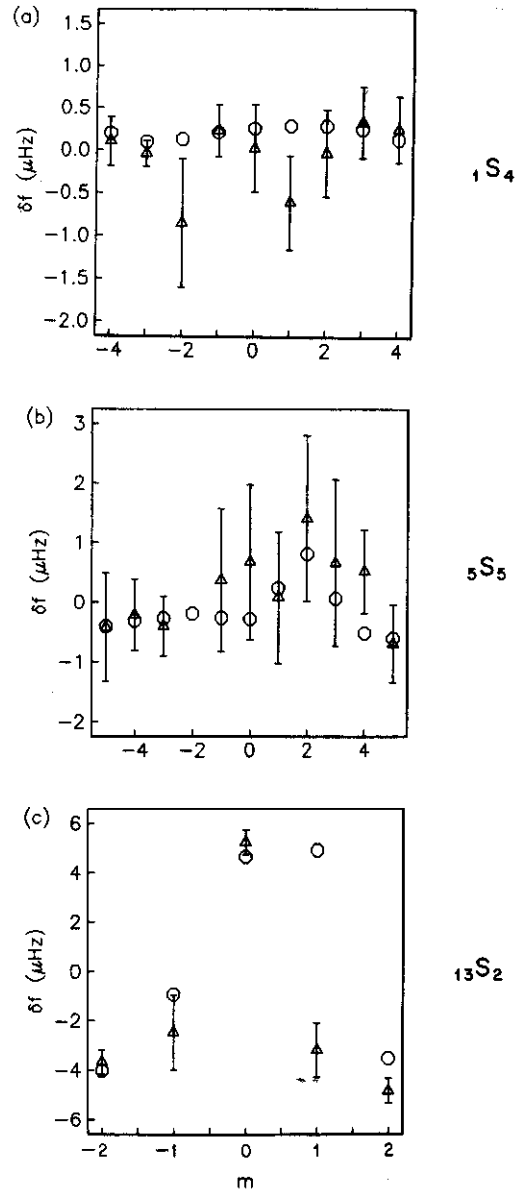

Fig. 11. Comparison between observed singlet frequencies from singlet stripping (triangles with 1σ errors) and nonlinear regression (octagons) for (*a*) ${}_1S_4$, (*b*) ${}_5S_5$, and (*c*) ${}_{13}S_2$. Frequencies are represented as perturbations to the frequencies predicted for a rotating, hydrostatic (RH) earth model. That is, $\delta f_m=\hat{f}_m-f_m^{RH}$, where $\hat{f}_m$ is the observed frequency and f_m^{RH} the predicted frequency for the RH model. Agreement for ${}_1S_4$ and ${}_5S_5$ is within 1σ for most singlets. Misfit for $m=+1$ singlet of ${}_{13}S_2$ is discussed in the text.

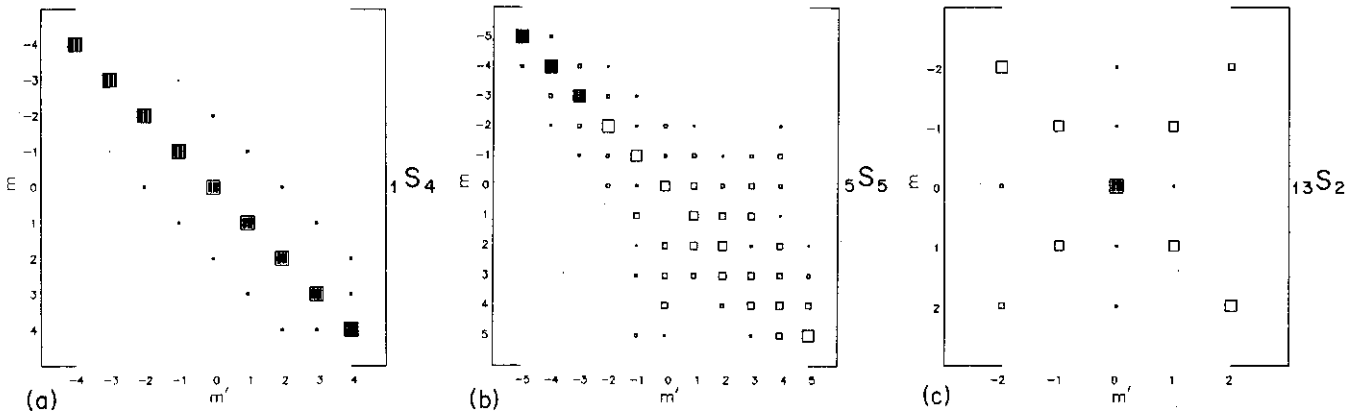

Fig. 12. Moduli of eigenvector matrices estimated by nonlinear regression for the three multiplets of Figure 11: (*a*) ${}_1S_4$, (*b*) ${}_5S_5$, and (*c*) ${}_{13}S_2$. The eigenvector matrix for ${}_5S_5$ is quite different from the identity matrix, indicating the robustness of the singlet frequencies estimated by singlet stripping to degradation caused by nonaxisymmetric heterogeneity. (See Figure 3*a* caption for plot description.)

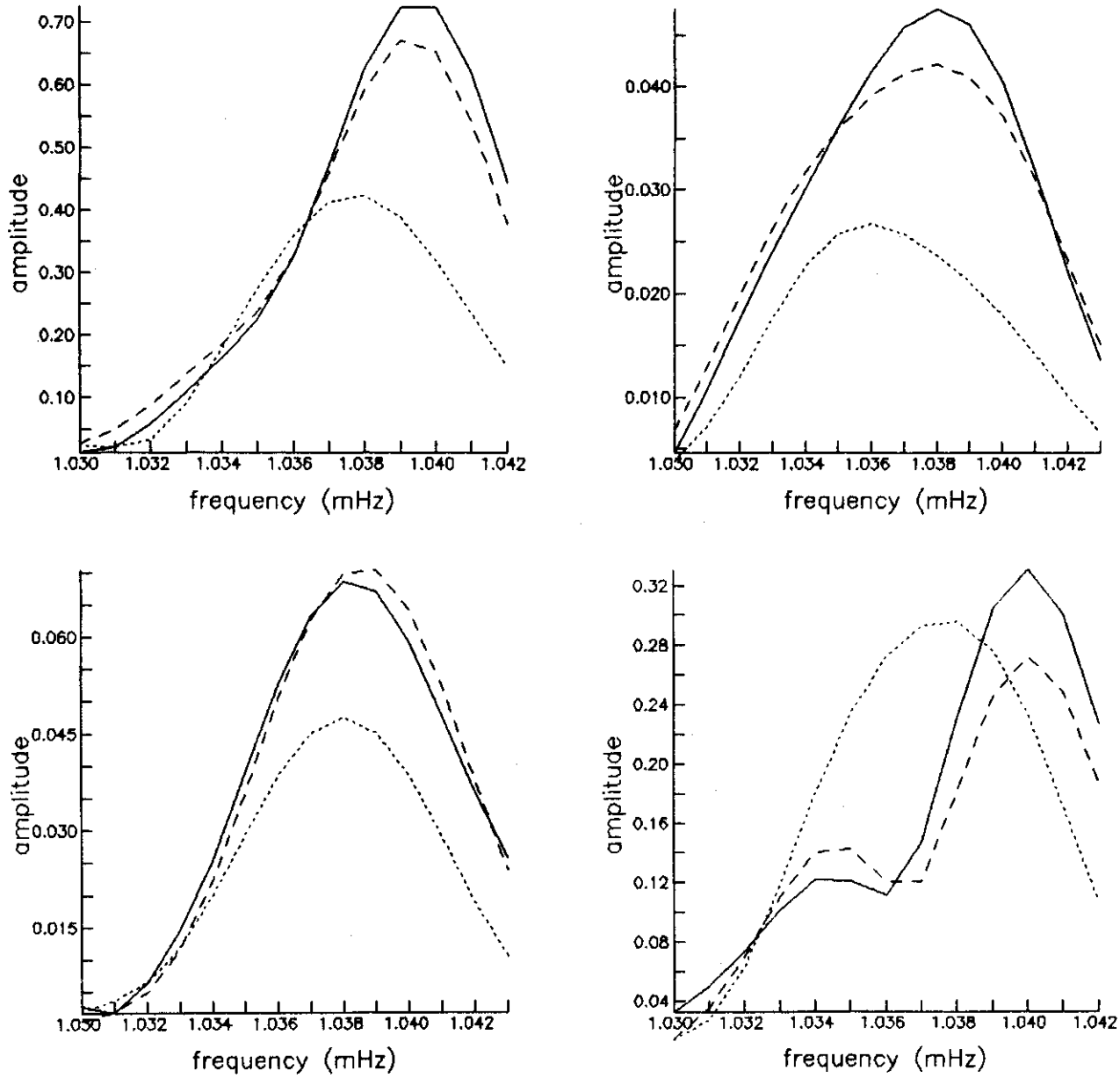

Fig. 13. Comparative fit to seismic amplitude spectra (solid line), in the narrow frequency band around ${}_0S_6$, by the synthetic seismogram produced by the c_2^0 estimated from singlet stripping (dotted line) and the synthetic produced by c_2^1 estimated by nonlinear regression. The nonaxisymmetric coefficients c_2^1 are [1.89, 0.39, 0.09, −2.43, 2.09] μHz and greatly improve the fit to the spectra. The recordings here are (clockwise from upper left): NNA 1977, 231; HAL 1979, 346; HAL 1977, 231; COL 1979, 346.

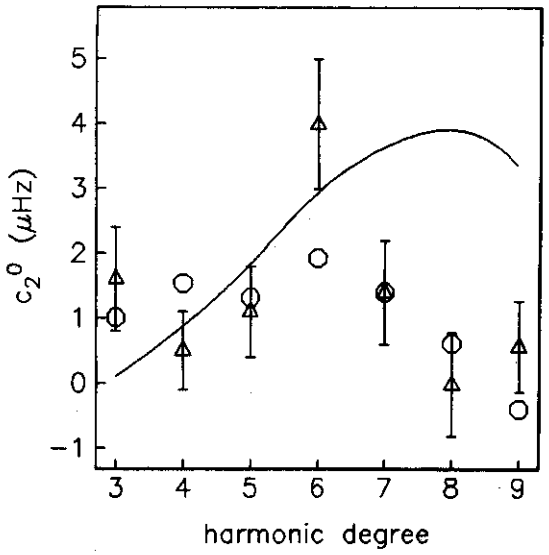

Fig. 14. The c_2^0 coefficients along fundamental mode branch. The estimate from singlet stripping (triangles) with 1σ errors agrees with the estimate from nonlinear regression (octagons) at the 2σ level. Worse misfit for ${}_0S_6$ probably is due to the expected bias in the singlet stripping estimate. The predicted c_2^0 coefficients for the hydrostatic core model, plotted as the solid line, misfit observations from both techniques for $l > 6$.

than the zonal degree 2 part of the lower mantle model estimated from P wave travel times by *Dziewonski* [1984]. A lower mantle structure as large as in our models should be seen in P and S wave travel time residuals of lower mantle phases. These problems clearly merit further

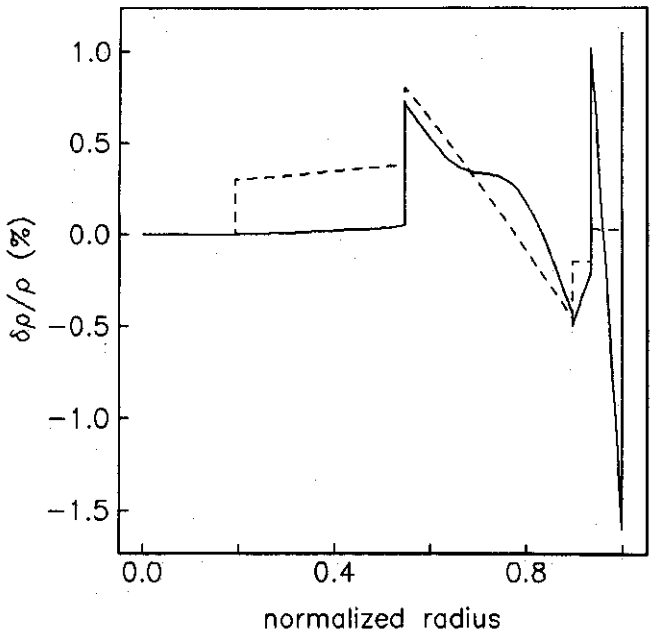

Fig. 15. Modeling results. Zonal perturbation in density relative to the radial earth model is plotted versus radius. Hydrostatic core model (solid line): only hydrostatic core structure allowed during inversion; nonhydrostatic core model (dashed line): outer core free during inversion. The fit to the estimated c_2^0 coefficients is summarized in Table 6 for each model. The sign of the Legendre function by which $\delta\rho_2^0$ is multiplied to give the angular dependence of each model implies that a negative $\delta\rho_2^0/\rho$ produces an ellipticity oriented with the hydrostatic ellipticity of figure.

TABLE 6. Fit to the 29 c_2^0 Estimates

Model	χ^2	Variance Reduction
RH model	580	—
Hydrostatic core model	195	66%
Nonhydrostatic core model	125	78%

investigation. We are currently applying the nonlinear regression to a large data set to refine our ability to model the aspherical structure of the deep earth.

7. Conclusions

The problem of inverting for the aspherical structure of the earth is complicated by the nonlinear dependence of low-frequency seismic waveforms on aspherical structure. We have developed two techniques which, in complementary ways, aim to overcome this obstacle. The first technique, called singlet stripping, estimates singlet resonance functions by linearly recombining many seismic recordings. Although large amounts of nonaxisymmetric earth structure degrade the resonance functions estimated by this technique, experiments with synthetic data show that the singlet frequencies determined from the resonance functions are surprisingly robust. The application of singlet stripping to many low harmonic degree, high-Q, multiplets has resolved approximately 290 singlets from 34 multiplets. A subset of these singlet frequency observations has been compared with the results from the second technique. This technique, a nonlinear regression, iteratively estimates coefficients which are linear functionals of aspherical structure and yields singlet frequencies in relative agreement with those from singlet stripping for most multiplets. Results from both techniques indicate that most of the multiplets resolved possess singlet frequency distributions in agreement with those predicted for a rotating earth model in hydrostatic equilibrium (RH model). However, the main result of this paper is that approximately a third are anomalously widely split, spanning frequency bands up to 2.5 times greater than predicted for an RH model. All the anomalously widely split multiplets are SKS, PKP, or PKIKP equivalent. The anomalous splitting width is a highly robust datum and provides compelling evidence for deep large-scale, nonhydrostatic aspherical structure.

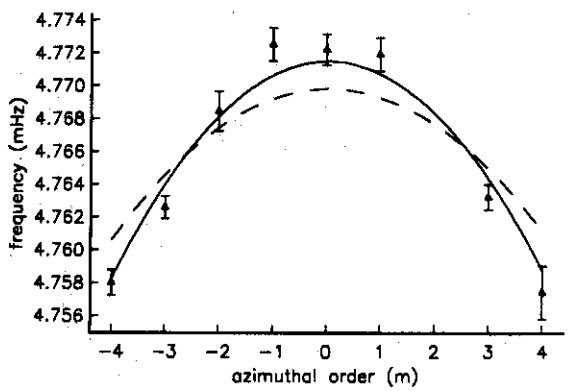

Fig. 16. Fit to the observed singlet frequencies of ${}_{11}S_4$ by the hydrostatic core model (dashed line) and the nonhydrostatic core model (solid line). The frequencies are systematically misfit unless nonhydrostatic structure is allowed in the core.

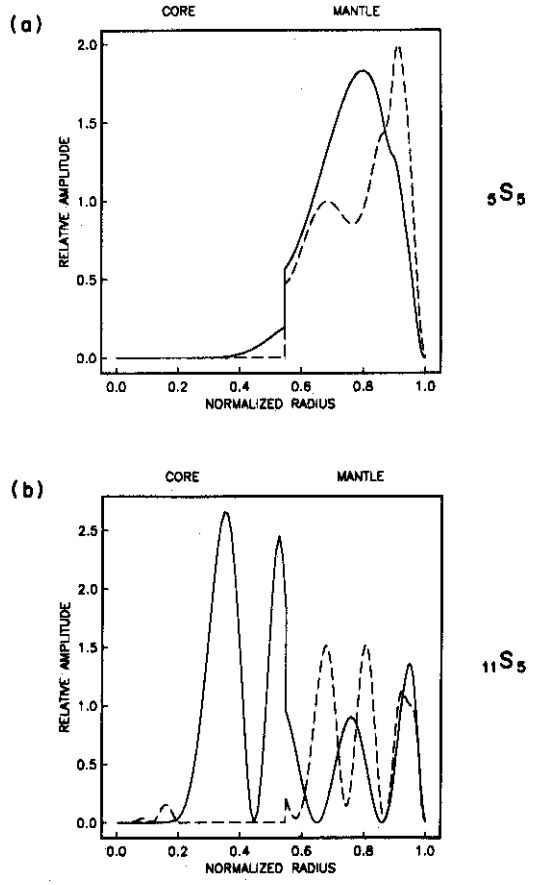

Figure 17. Compressional (solid line) and shear (dashed line) elastic energy densities versus radius for (*a*) the normally split multiplet $_5S_5$ and (*b*) the anomalously wide multiplet $_{11}S_5$. Like all anomalously wide multiplets, $_{11}S_5$ possesses its classical turning point and, therefore, large energy densities in the core.

The axisymmetric aspherical structure coefficients, c_2^0, which we infer from the observed singlet frequencies, apparently can be biased by up to two standard deviations due to the possible presence of large nonaxisymmetric structure. Nevertheless, many of the c_2^0 coefficients are significantly different from zero (by several standard deviations). A direct inversion indicates that to explain the splitting widths of the SKS, PKP, and PKIKP equivalent multiplets, aspherical structure would have to be large and oscillatory if confined to the mantle. The observed singlet frequencies can, however, be reasonably well fit by a model which is smooth in the mantle if a relatively large amount of nonhydrostatic structure is included in the outer core. There are good theoretical reasons for believing that such an outer core structure is geophysically unreasonable, yet it is interesting to note that differential travel time data, which are sensitive to the properties of the lower outer core and inner core, apparently also require large-scale variations in structure not unlike those reported here. The splitting characteristics of many more multiplets than we have considered here are amenable to investigation using spectral fitting techniques like the nonlinear regression, and it is not unreasonable to predict that reliable models of the large scale aspherical structure of the deep earth will be available in the near future.

APPENDIX: RAPID CALCULATION OF THE DIFFERENTIAL SEISMOGRAMS

The application of the nonlinear regression to estimate the c_s^i coefficients (section 3.2) requires the calculation of the differential seismograms in (12). For a single isolated multiplet (fixed k), we follow *Woodhouse and Girnius* [1982] and rewrite (4) as

$$\mathbf{s}(t) = \boldsymbol{\sigma}^T \mathbf{a}(t) e^{i\omega t} \tag{A1}$$

where the real part is assumed. The envelope function $\mathbf{a}(t)$ is given by

$$\mathbf{a}(t) = \mathbf{P}(t)\mathbf{a}\,, \qquad \mathbf{a}(0) = \mathbf{a} \tag{A2}$$

where $\mathbf{P}(t) = e^{i\mathbf{H}t}$ is the matrizant or propagator matrix of the following first-order homogeneous propagator equation with initial condition given in (A2):

$$\frac{d}{dt}\mathbf{a}(t) = i\mathbf{H}\mathbf{a}(t) \tag{A3}$$

In practice, we will only need to calculate $\mathbf{P}(\delta t)$ which is well enough conditioned so that both spectral decomposition (A4*a*) and series expansion (A4*b*) are satisfactory:

$$\mathbf{P}(\delta t) = \mathbf{U} e^{i\Omega \delta t} \mathbf{U}^{-1} \tag{A4a}$$

$$\equiv \sum_{n=0}^{n_{\max}} \alpha_n \quad \text{where} \quad \alpha_n = \frac{i\delta t}{n}\mathbf{H}\alpha_{n-1}\,, \quad \alpha_0 = \mathbf{I} \tag{A4b}$$

Let $\mathbf{d}_j(t) = \partial \mathbf{a}(t)/\partial c_j$, then the differential seismogram for the jth coefficient is

$$\frac{\partial \mathbf{s}(t)}{\partial c_j} = \boldsymbol{\sigma}^T \mathbf{d}_j(t) e^{i\omega t} \tag{A5}$$

We present two algorithms for rapidly calculating $\mathbf{d}_j(t)$ and hence the differential seismograms in (A5).

Recursion Relation in Time

Equation (A2) can be rewritten as a recursion relation in time:

$$\mathbf{a}(t+\delta t) = \mathbf{P}(\delta t)\mathbf{a}(t) \tag{A6}$$

from which a recursion relation for $\mathbf{d}_j(t)$ follows directly:

$$\mathbf{d}_j(t+\delta t) = \mathbf{Q}_j(\delta t)\mathbf{a}(t) + \mathbf{P}(\delta t)\mathbf{d}_j(t)\,, \quad \mathbf{d}_j(0) = 0 \tag{A7}$$

where, by (A4*b*),

$$\mathbf{Q}_j(\delta t) = \frac{\partial}{\partial c_j}\mathbf{P}(\delta t)$$

$$= i\delta t \boldsymbol{\Gamma}_j + \frac{(i\delta t)^2}{2}(\mathbf{H}\boldsymbol{\Gamma}_j + \boldsymbol{\Gamma}_j\mathbf{H}) + \cdots$$

$$= \sum_{n=0}^{n_{\max}} \boldsymbol{\beta}_{nj}$$

with

$$\boldsymbol{\beta}_{nj} = \frac{i\delta t}{n}(\boldsymbol{\Gamma}_j \boldsymbol{\alpha}_{n-1} + \mathbf{H}\boldsymbol{\beta}_{(n-1)j})\,, \quad \boldsymbol{\beta}_{0j} = 0$$

and

$$\boldsymbol{\Gamma}_j = \frac{\partial}{\partial c_j}\mathbf{H} \tag{A8}$$

By (A7), $\mathbf{d}_j$ can be propagated in time and then combined with (A5) to form the differential seismogram associated with each c_j.

Inhomogeneous Propagator Formalism

A nonrecursive algorithm for computing $\mathbf{d}_j(t)$ can be found. Differentiating (A3) with respect to c_j and using (A8):

$$\frac{d}{dt}\mathbf{d}_j(t) = i(\mathbf{H}\mathbf{d}_j(t) + \mathbf{\Gamma}_j\mathbf{a}(t)) \tag{A9}$$

Equation (A9) is an inhomogeneous propagator equation which can be solved immediately with the initial condition given in (A7) [*Gilbert and Backus*, 1966, equation (2.7)]:

$$\mathbf{d}_j(t) = i\left[\int_0^t \mathbf{P}(t-\tau)\mathbf{\Gamma}_j\mathbf{P}(\tau)d\tau\right]\mathbf{a}$$

$$= \mathbf{U}\mathbf{\Delta}_j(t)\mathbf{U}^{-1}\mathbf{a} \tag{A10}$$

where the latter equality follows by (A4*a*) and where

$$\mathbf{\Delta}_j(t) = i\int_0^t e^{i\Omega(t-\tau)}\mathbf{W}_j\, e^{i\Omega\tau}d\tau$$

with

$$\mathbf{W}_j = \mathbf{U}^{-1}\mathbf{\Gamma}_j\mathbf{U} \tag{A11}$$

The $(p,q)^{\text{th}}$ component of $\mathbf{\Delta}_j$ can be computed directly:

$$\Delta_{jpq}(t) = W_{jpq}F_{pq}(t) \quad \text{(no summation)} \tag{A12}$$

with

$$F_{pq}(t) = i\int_0^t e^{i\Omega_p(t-\tau)}e^{i\Omega_q\tau}d\tau$$

$$= \begin{cases} \dfrac{e^{i\Omega_p t} - e^{i\Omega_q t}}{\Omega_p - \Omega_q} & \text{if } p \neq q \\ ite^{i\Omega_p t} & \text{if } p = q \end{cases} \tag{A13}$$

Equations (A10)–(A13) can now be combined with (A5) to form the differential seismogram for each coefficient c_j.

The recursion relation is marginally faster than the propagator formalism. In either case, however, since $\mathbf{d}_j(t)$ is much more slowly varying that $e^{i\omega t}$, $\mathbf{d}_j(t)$ need only be calculated on a coarse time grid and interpolated later for multiplication with $e^{i\omega t}$. Since $\mathbf{d}_j(t)$ is receiver independent, it need only be computed once per seismic event.

Acknowledgments. We thank J. Park and R. Woodward for many valuable discussions. We thank T. H. Jordan for bringing to our attention the PKP and PKIKP travel time anomalies. We thank both the IDA and GDSN organizations for providing us with high quality digital data and, also, L. Knopoff for making available some important South Pole recordings of large events. Our research has been supported by National Science Foundation grants EAR-80-2561, EAR-81-21866, and EAR-84-10369.

REFERENCES

Anderson, O. L., E. Schreiber, R. C. Lieberman, and M. Soga, Some elastic constant data on minerals relevant to geophysics, *Rev. Geophys., 6*, 491–524, 1968.

Backus, G. E., Converting vector and tensor equations to scalar equations in spherical coordinates, *Geophys. J. R. Astron. Soc., 13*, 71–101, 1967.

Backus, G. E., and F. Gilbert, Rotational splitting of the free oscillations of the earth, *Proc. Natl. Acad. Sci. U.S.A., 47*, 362–371, 1961.

Benioff, H., F. Press, and S. W. Smith, Excitation of the free oscillations of the earth by earthquakes, *J. Geophys. Res., 66*, 605–619, 1961.

Bolt, B. A., and D. R. Brillinger, Estimation of uncertainties in eigenspectral estimates from decaying geophysical time series, *Geophys. J. R. Astron. Soc., 59*, 593–603, 1979.

Buland, R., and F. Gilbert, Improved resolution of complex eigenfrequencies in analytically continued seismic spectra, *Geophys. J. R. Astron. Soc., 52*, 457–470, 1978.

Chao, B. F., and F. Gilbert, Autoregressive estimation of complex eigenfrequencies in low frequency seismic spectra, *Geophys. J. R. Astron. Soc., 63*, 641–657, 1980.

Buland, R., J. Berger, and F. Gilbert, Observations from the IDA network of attenuation and splitting during a recent earthquake, *Nature, 277*, 358–362, 1979.

Clayton, R. W., and R. P. Comer, A tomographic analysis of mantle heterogeneities from body wave travel times (abstract), *Eos Trans. AGU, 64*, 776, 1983.

Creager, K. C., and T. H. Jordan, Large scale structure of the outermost core from P'_{DF} and P'_{AB} travel times, *Eos Trans. AGU, 67*, 311, 1986.

Dahlen, F. A., The normal modes of a rotating, elliptical earth, *Geophys. J. R. Astron. Soc., 16*, 329–367, 1968.

Dahlen, F. A., The normal modes of a rotating, elliptical earth, II, Near resonant multiplet coupling, *Geophys. J. R. Astron. Soc., 18*, 397–436, 1969.

Dahlen, F. A., Reply, *J. Geophys. Res., 81*, 491, 1976.

Dahlen, F. A., The effect of data windows on the estimation of free oscillation parameters, *Geophys. J. R. Astron. Soc., 69*, 537–549, 1982.

Dahlen, F. A., and R. V. Sailor, Rotational and elliptical splitting of the free oscillations of the earth, *Geophys. J. R. Astron. Soc., 58*, 609–623, 1979.

Dziewonski, A. M., Mapping the lower mantle: Determination of lateral heterogeneity in *P* velocity up to degree and order 6, *J. Geophys. Res., 89*, 5929–5952, 1984.

Dziewonski, A. M., and F. Gilbert, Observations of normal modes from 84 recordings of the Alaskan earthquake of 28 March 1964, II, *Geophys. J. R. Astron. Soc., 35*, 401–437, 1973.

Dziewonski, A. M., T. A. Chou, and J. H. Woodhouse, Determination of the earthquake source parameters from waveform data for studies of global and regional seismicity, *J. Geophys. Res., 86*, 2825–2853, 1981.

Edmonds, A. R., *Angular Momentum and Quantum Mechanics*, Princeton University Press, Princeton, N.J., 1960.

Gilbert, F., The diagonal sum rule and averaged eigenfrequencies, *Geophys. J. R. Astron. Soc., 23*, 125–128, 1971.

Gilbert, F., and G. Backus, Propagator matrices in elastic wave and vibration problems, *Geophysics, 31*, 326–332, 1966.

Gilbert, F., and A. M. Dziewonski, An application of normal mode theory to the retrieval of structural parameters and source mechanisms from seismic spectra, *Philos. Trans. R. Soc. London, Ser. A, 278*, 187–269, 1975.

Gilbert, F., A. M. Dziewonski, and J. Brune, An informative solution to a seismological inverse problem, *Proc. Natl. Acad. Sci., U.S.A., 70*, 1410–1413, 1973.

Golub, G., and C. Reinsch, Singular value decompositions and least squares solutions, in *Linear Algebra*, edited by J. H. Wilkinson and C. Reinsch, pp. 134–151, Springer-Verlag, New York, 1971.

Hager, B. H., R. W. Clayton, M. A. Richards, R. P. Comer, and A. M. Dziewonski, Lower mantle heterogeneity, dynamic topography, and the geoid, *Nature, 313*, 541–545, 1985.

Hansen, R. A., Simultaneous estimation of terrestrial eigenvibrations, *Geophys. J. R. Astron. Soc., 70*, 155–172, 1982.

Johnston, J., *Econometric Methods*, 3rd ed., pp. 259–264, McGraw-Hill, New York, 1984.

Luh, P. C., Free oscillations of the laterally inhomogeneous earth:

Quasi-degenerate multiplet coupling, *Geophys. J. R. Astron. Soc., 32*, 187–202, 1973.

Luh, P. C., The normal modes of the rotating self-gravitating inhomogeneous earth, *Geophys. J. R. Astron. Soc., 38*, 187–224, 1974.

Madariaga, R., Free oscillations of the laterally heterogeneous earth, Ph.D. thesis, 105 pp., Mass. Inst. of Technol., Cambridge, 1971.

Masters, G., and F. Gilbert, Structure of the inner core inferred from observations of its spheroidal shear modes, *Geophys. Res. Lett., 8*, 569–571, 1981.

Masters, G., and F. Gilbert, Attenuation in the earth at low frequencies, *Philos. Trans. R. Soc. London, Ser. A, 308*, 479–522, 1983.

Masters, G., T. H. Jordan, P. G. Silver, and F. Gilbert, Aspherical earth structure from fundamental spheroidal-mode data, *Nature, 298*, 609–613, 1982.

Masters, G., J. Park, and F. Gilbert, Observations of coupled spheroidal and toroidal modes, *J. Geophys. Res., 88*, 10,285–10,298, 1983.

Morris, S. P., H. Kawakatsu, R. J. Geller, and S. Tsuboi, A calculation of the normal modes of realistic laterally heterogeneous, anelastic earth models at 250 sec period (abstract), *Eos Trans. AGU, 65*, 1002, 1984.

Nakanishi, I., and D. L. Anderson, Measurements of mantle wave velocities and inversion for lateral heterogeneity and anisotropy, 1, Analysis of great circle phase velocities, *J. Geophys. Res., 88*, 10,267–10,283, 1983.

Nakanishi, I., and D. L. Anderson, Measurement of mantle wave velocities and inversion for lateral heterogeneity and anisotropy, II, Analysis by the single-station method, *Geophys. J. R. Astron. Soc., 78*, 573–618, 1984.

Nakiboglu, S. M., Hydrostatic theory of the earth and its mechanical implications, *Phys. Earth Planet. Inter., 28*, 302–311, 1982.

Ness, N. F., C. J. Harrison, and L. J. Slichter, Observations of the free oscillations of the earth, *J. Geophys. Res., 66*, 621–629, 1961.

Park, J., and F. Gilbert, Coupled free oscillations of an aspherical, dissipative, rotating earth: Galerkin theory, *J. Geophys. Res., 91*, 7241–7260, 1986.

Pekeris, C. L., A. Alterman, and M. Jarosch, Rotational multiplets in the spectrum of the earth, *Phys. Rev., 122*, 1692–1700, 1961.

Poupinet, G., R. Pillet, and A. Souriau, Possible heterogeneity of the earth's core deduced from PKIKP travel times, *Nature, 305*, 204–206, 1983.

Schulten, K., and R. Gordon, Exact recursive evaluation of 3-*j* and 6-*j* coefficients for quantum mechanical coupling of angular momenta, *J. Math. Phys., 16*, 1961–1970, 1975.

Stein, S., and R. Geller, Amplitude for the split normal modes of a rotating, elliptical earth excited by a double couple, *J. Phys. Earth, 25*, 117–142, 1978.

Tanimoto, T., and B. A. Bolt, Coupling of torsional modes in the earth, *Geophys. J. R. Astron. Soc., 74*, 83–96, 1983.

Thomson, D. J., Spectrum estimation and harmonic analysis, *IEEE Proc., 70*, 1055–1096, 1982.

Woodhouse, J. H., On Rayleigh's principle, *Geophys. J. R. Astron. Soc., 46*, 11–22, 1976.

Woodhouse, J. H., The coupling and attenuation of nearly resonant multiplets in the earth's free oscillation spectrum, *Geophys. J. R. Astron. Soc., 61*, 261–283, 1980.

Woodhouse, J. H., and F. A. Dahlen, The effect of a general aspherical perturbation on the free oscillations of the earth, *Geophys. J. R. Astron. Soc., 53*, 335–354, 1978.

Woodhouse, J. H., and A. M. Dziewonski, Mapping the upper mantle: Three-dimensional modeling of earth structure by inversion of seismic waveforms, *J. Geophys. Res., 89*, 5953–5986, 1984.

Woodhouse, J., and D. Giardini, Inversion for the splitting function of isolated low order normal mode multiplets, (abstract) *Eos Trans. AGU, 66*, 300, 1985.

Woodhouse, J. H., and T. P. Girnius, Surface waves and free oscillations in a regionalized earth model, *Geophys. J. R. Astron. Soc., 68*, 653–673, 1982.

Zharkov, B. N., and V. M. Lyubimov, Theory of spheroidal vibrations for a spherically asymmetrical model of the earth, *Izv. Acad. Sci. USSR Phys. Solid Earth, no. 10*, 613–618, 1970.

F. Gilbert, G. Masters, and M. Ritzwoller, Institute of Geophysics and Planetary Physics, Scripps Institution of Oceanography, University of California, San Diego, La Jolla, CA 92093.

(Received May 13, 1985;
revised April 8, 1986;
accepted May 13, 1986.)